A Dissertation Report
On

Numerical Analysis of Steel-Concrete Composite Girder Under Cyclic Loading

Submitted in Partial Fulfilment of the Requirements for the Award of Degree of

MASTER OF TECHNOLOGY
IN
STRUCTURAL ENGINEERING

Submitted by
ASHUTOSH GUPTA
(2015PCS5237)

To

DEPARTMENT OF CIVIL ENGINEERING
MALAVIYA NATIONAL INSTITUTE OF TECHNOLOGY,
JAIPUR-302017-RAJASTHAN (INDIA)

APRIL 2016

A Dissertation Report
On

Numerical Analysis of Steel-Concrete Composite Girder Under Cyclic Loading

Submitted in Partial Fulfilment of the Requirements for the Award of Degree of

MASTER OF TECHNOLOGY
IN
STRUCTURAL ENGINEERING

Submitted by
ASHUTOSH GUPTA
(2015PCS5237)

To

DEPARTMENT OF CIVIL ENGINEERING
MALAVIYA NATIONAL INSTITUTE OF TECHNOLOGY,
JAIPUR-302017-RAJASTHAN (INDIA)
APRIL 2016

MALAVIYA NATIONAL INSTITUTE OF TECHNOLOGY JAIPUR

MALAVIYA NATIONAL INSTITUTE OF TECHNOLOGY JAIPUR

Certificate

I hereby certify that the work which is being presented in dissertation entitled "**Numerical Analysis of Steel-Concrete Composite Girder Under Cyclic Loading**" is an authentic record of my own work, carried out under the supervision of Dr Sandeep Chaudhary Associate Professor, in partial fulfilment of the requirements for the award of **Degree of Master of Technology** in **Department of Civil Engineering** from Malaviya National Institute of Technology, Jaipur for the year 2015-17.

Ashutosh Gupta
(2015PCS5237)
IVth Sem, M. Tech.

This is to certify that the above statement made by the candidate is correct to the best of my/our knowledge.

Dr Sandeep Chaudhary
Department of Civil Engineering
Malaviya National Institute of Technology Jaipur
Jaipur

ACKNOWLEDGEMENT

It is a matter of great pleasure and privilege for me to present this dissertation on "**Numerical Analysis of Steel-Concrete Composite Girder under Cyclic Loading."** I take this opportunity to express my deep sense of gratitude and respect towards my guide **Dr. Sandeep Chaudhary,** Department of Civil Engineering, Malaviya National Institute of Technology, Jaipur. I am very much indebted to him for the generosity, expertise, and guidance which I have received from him working on this dissertation and throughout my studies.

I would like to thank **Dr. Gunwant Sharma**, Professor, and Head of the Department of Civil Engineering, Malaviya National Institute of Technology, Jaipur for giving me this opportunity to do this work and all the staff members of the Department of Civil Engineering for their constant encouragement.

I would also like to express my gratitude towards P.G. Coordinator **Dr. Vinay Agrawal** who helped me for the completion of my dissertation and **Mr. Pankaj Kumar** for his effective guidance.

Last but never the least sincere thanks go to all my friends who have helped me and encouraged me for successfully completing this work.

ASHUTOSH GUPTA

(2015PCS5237)

IVth Sem Mtech.

ABSTRACT

Steel-concrete composite bridges are commonly used all over the world owing to the fact they offer many advantages, comprising high strength to self -weight ratio, speed of construction, repair and recycle and durability. Steel and Concrete behaviour are dependents on their load history of reversal cycles. In this research work, Numerical Analysis of fully scale simply supported steel- concrete composite girder under cyclic loading is performed. A Steel- Concrete Composite girder with headed shear stud connectors is modelled using finite element modelling tools and analysed its true non-linear response under various number of cycles. Numerical simulations are also performed on the composite beam by loading statically up to the load at failure and at peak cyclic load to assess its behaviour under static analysis and further compared its response under cyclic loading. Cyclic tests were performed subjecting the composite beam to various number of cycles mainly 25 cycles and 100 cycles with its peak cyclic load adopted between yield load and ultimate load capacity to assess the non-linear behaviour of steel and concrete. Various parameters such as stress and strain of concrete and steel at peak cyclic load, mid-span deflection are investigated for the numerical analysis under cyclic loading. The results of cyclic tests at peak cyclic load are compared with those obtained with the static analysis and shows decrease in mid-span deflections, stress and strain of steel and increase in that of concrete at peak cyclic load. The stress vs. strain graph for concrete under cyclic loading shows the increase in ultimate strain with the increase in the accumulated residual strain. The stress vs. strain graph for steel under cyclic loadings represents a event where plastic deformation ceases after one cycle and the response goes back to pure elastic with some state of residual stress. The unloading and the reloading curves coincide and are parallel to the initial loading curve. Residual stress and steel for concrete and steel are tensile in nature, increases with the number of cycles and finally become constant.

Table of Contents

List of Figures

List of Tables

CHAPTER 1

INTRODUCTION

1.1 General

A composite material is generally defined as a mixture of two or more materials that leads in enhancing the properties than those of the individual material used alone. Generally in reference to metallic alloys, each constituents holds its distinguish chemical, physical, and mechanical properties. The two distinguished constituents in composite materials are a reinforcement and a matrix. Some of the main benefits of composite materials are their increase in strength and stiffness with reduction in unit weight of the composite as compared with bulk materials, resulting into the mass reduction in the finished part. Any part of the structure or component which is designed on the basis of carrying a single monotonically increasing static load may collapse or fail in the application of same load or even smaller load if applied cyclically for large number of times. Cyclic loading is the application of stresses, strains, or stress intensities in reversal or fluctuating waves at the considered locations on the structural components. Due to reversal or fluctuation of stress, strain or any property, the degradation of material takes place which may occur at the considered locations leads to fatigue degradation (Hoeppner 2013). 3-Dimensional Finite element analysis enables us to access the variation of different parameters like stress, strain, bending moment, etc. across the length, width and depth of the structure. Abaqus is a Finite element modeling tool which is used for modelling, analysis, assemblies and visualizing the results to predict the true behaviour of engineering structures (Hibbitt et al. 2013). Many researchers have used Abaqus to model the steel bridges, reinforced concrete bridges, steel concrete composite girder to analyse the behaviour of them as it gives the elemental analysis of the model and is capable of assessing the exact response of the model.

1.2 Steel Concrete Composite Girder

Steel-concrete composite bridges are commonly used all over the world owing to the fact they offer many advantages, comprising high strength to self-weight ratio, the speed of construction, repair and recycle and durability. Steel-concrete composite beams comprises of a steel beam and a reinforced concrete slab which is cast in-situ and placed over it held together by the mechanical connectors mainly shear connectors or by adhesive bonded connections (Mishra 2009). A steel concrete composite beam is generally used to increase its flexural rigidity, moment carrying capacity of the structure. If concrete slabs are just placed over steel beams and supported by them, it may leads both concrete and steel members to act independently. Due to such conventional composite construction, slip may occurs between them as there is no connection between them leads to failure of either concrete or steel members. For elimination of slip between them, a shear connector or adhesive bonded connection must be provided between concrete slab and steel beam to act as a composite beam. Composite action between steel and concrete enables both to achieve its both material advantages. Conrete is stronger in compression but weaker in tension

whereas steel is stronger in tension but susceptible to buckling phenomena, this weakness can be overcome by composite action. Composite steel beams shows less deflection as compared to steel construction due to its higher stiffness achieved through composite action. More economical section is achieved as compared to steel construction for the same span and the loading. A steel- concrete composite girder bridge of span 32m having a skew angle of 12 degree in Tamil Nadu at Singaperamolkovil Railway station near district Chengalpet is the south India longest composite bridge in which stresses over Square And Skew Span on composite bridge is studied. The composite girder provided several advantages as it had reduced the use of concrete as well as steel, offered higher strength, lessened floor sections and greater speed of construction (Ameeruthen and Aravindan 2014).

1.3 Connections

The steel–concrete composite member is more stiffer and has higher moment carrying capacity than steel beam and concrete slab alone. The main hindrance being connection at steel–concrete interface. The main purposes of a connection can include to transfer load, restrain movement, or to provide stability. Some of the connections include the use of headed studs, threaded rods, different types of anchors, and steel embedded members. The two materials are structurally tied together to carry compression for the concrete part within the effective width of the cross-section and to carry tension for the steel part (BCSA 2001). Steel-concrete composite beams comprising of two materials, concrete section which is placed over steel section must be tied togther by mechanical connectors to achieve composite action between them (Mahmoud 2016). One type of these connectors is called head studs as shown in figure below. The main purposes of these headed shear studs are to achieve joint behaviour of the beam-slab, to resist slipping and uplifting between the steel and concrete members and to carry shear forces (Kumar et al. 2016). The headed part of the shear stud is embedded into the concrete slab whereas base of it is welded to the top flange of the steel member.

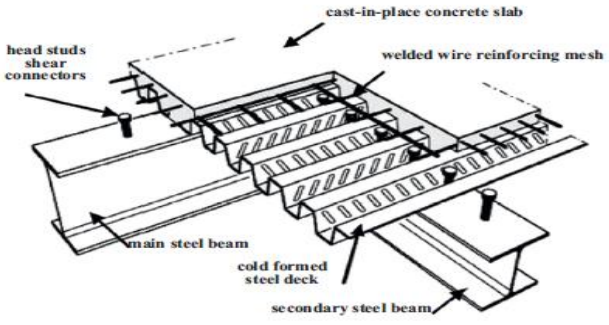

Figure 1.1 Illustrative sketch of roof slab with composite action (Mahmoud 2016)

Another connection or constraint is provided is Embedded Connection. In steel concrete composite girder stud and reinforcement are embedded into concrete deck slab. Reinforced concrete contains steel embedded in the concrete so the two materials

counterpart each other to resist forces such as tensile, shear and compressive stress in the concrete structure. Normal plain concrete can withstand compressive stress but does not do well with tensile and stresses such as those caused by wind, earthquakes and vibrations (Services 2007). In reinforced concrete it is necessary to develop bond action between the steel reinforcement and the concrete. Bond action ensures no slippage between the steel bars and the concrete surrounding it, confirms transfer of stress across the steel-concrete. Bond action is achieved through the adhesion, friction and mechanical interlock between steel and concrete surrounding it. A loss of bond action between the concrete and reinforcement may lead to failure of the structure. Connection details should recognize the physical characteristics of both steelwork and the material to which the steelwork is connected. The design of connection between steel and other materials must consider durability and maintenance aspects, long terms deflections and movements and variable property aspects of the materials.

Another connection between steel beam and concrete deck slab is Adhesive Bonded that can replace the need of Mechanical Connectors. Mechanical connectors, which have relatively higher value of slip such as stud, angle, channel, perfobond etc. are considered as flexible or semi-rigid connection and adhesively bonded connections are considered as rigid connection.(Kumar et al. 2017). Steel–concrete composite structures are progressively used in bridges or building due to its reduced cost of the construction. If there is possibility to improve the concrete resistance against cracking at an early age and reduce the cost of the materials, their use may further rise in the future. Adhesive bonded Connection provides more resistance for crack initiation as compared to mechanical connectors. Various adhesives are Polyurethane, Epoxy and so many more.

1.4 Organisation of Thesis

Chapter 1: Introduction

A brief introduction of composite materials, cyclic loading, steel-concrete composite girder and connections to be provided between steel and concrete parts of the composite girder.

Chapter 2: Literature Review

The previous studies referring to the modelling of steel-concrete composite girder and cyclic tests on composite girder has been reviewed in this chapter. The research gap in the current studies has been revealed and based upon that gap an objective has been presented.

Chapter 3: Methodology

This chapter deals with the methodology developed for modelling and analysis of steel-concrete composite girder under cyclic loading.

Chapter 4: Numerical Validation

This chapter deals with validation of steel and concrete material properties using finite element modelling of previous researches on composite girders.

Chapter 5: Results and Discussions

The results obtained from the numerical analysis of composite girder are precisely presented and discussed in this chapter with the help of figures.

Chapter 6: Conclusion

The conclusion formed on the basis of the results obtained along with future scope of work are discussed in this chapter.

CHAPTER 2

LITERATURE REVIEW

2.1 Overview

The previous studies referring to the finite element analysis of steel-concrete composite girder and behaviour of concrete and steel subjected to cyclic test have been reviewed.

Zhao and Li (2008) investigated the non-linear behaviour and the failure mechanism of the epoxy bonded steel-concrete composite beam using finite element modelling tools. For the analysis of the composite girder, threee-dimensional modelling of the parts are done. The composite beam of span length 3.5 m is simply supported at ends and loaded at the mid-span on the upper surface of the slab with the loaded area of 80 × 80 mm^2 for analysis. Zhao and Li (2008) used the Finite element program Abaqus to simulate the structural behavior of the composite beam. The composite girder is modelled only one-quarter due to the symmetry of the load application, boundary conditions and cross-sectional geometry about the centerline of the girder. Steel beam and concrete slab are modelled with eight-node brick element (C3D8) whereas adhesive layer is assigned eight-node three- dimensional cohesive element (COH3D8). Stress-strain relationship for the steel-beam and the steel bars are designated by trilinear curve and bilinear curve respectively. The stress vs. strain relationship proposed by Carreira and Chu (1985) has been used to model the elastic–plastic behaviour of concrete in the compression stage with strain softening. In this paper, ultimate compressive strain is 0.003, modulus of elasticity is 36,600 MPa. The stress vs. strain curve for concrete in compression is assumed to be linear until 0.4 times the maximum compressive strength of the concrete, beyond this concrete is in the plastic region. The stress vs. strain curve for concrete in tensile is assumed to be linearly increasing with the strain until the crack appears, afterwards stress to be linearly decreases and reaches zero with tensile strain reaches to a value of total strain.

Zheng et al. (2009) analysed the structural behaviour of concrete bridge deck slabs with patch loads applied statically on composite bridges by finite element analysis. A nonlinear 3-Dimensional finite element analysis model was developed using finite element software Abaqus. The concrete bridge deck slabs, steels supporting beams and diaphragms are modelled using shell elements (S4R or S8R). Composite action was assumed to develop between steel beams and concrete deck slab, achieved using multipoint constraint between the top steel flanges and concrete deck slab assuring nodal compatibility at the locations. The nonlinear behaviour of steel used as structural steel in beams and reinforcement bars has been designated using bilinear stress-strain curve. The tensile behaviour of concrete has been modelled using the tension stiffening model. Post failure behaviour of concrete in tension is defined using tension softening model. Concrete damage plasticity model is used to account for the nonlinear behaviour of concrete under compression. In conclusion, analysis results are discussed, along with inferences on the behaviour of the concrete deck slabs of bridges are presented.

Liang et al. (2005) uses finite element method to determine the flexural and shear strengths of composite beams simply supported at ends subjected to combined shear and bending. The composite beam has been modelled with three-dimensional finite elements to account for geometric and non-linear behaviour of materials, and the results are verified by experimental test. The concrete and steel beam elements are modelled using four-node doubly curved thick/thin shell elements with reduced integration. Stud shear connectors are modelled with three-dimensional beam elements. The nonlinear behaviour of steel material is analysed using von Mises yield criterion to account its plasticity. The stress vs. strain relationship in tension and compression for structural steel sections is designated using bilinear curves to account the non-linear behaviour of the steel material. The stress-strain curve must take account of material properties such as modulus of elasticity, yield stress, stress and strain at ultimate load and poisson's ratio. The compressive behaviour of concrete shows elastic-plastic behaviour with strain softening. The stress vs. strain relationship proposed by Carreira and Chu (1985) has been used to model the elastic–plastic behaviour of concrete in the uniaxial compression stage with strain softening. The stress–strain curve of concrete in uniaxial compression is assumed to be linear elastic up to 0.4 times the maximum compressive strength of the concrete. The strain at maximum compressive stress is taken as 0.002. A stress-strain curve for concrete having compressive strength of 42.5 MPa is achieved using mathematical equations. Tension-stiffening models is used to define the behaviour between the steel bars and concrete surrounded it. In tension stiffening model it is assumed that direct stress across the crack tends to zero as the crack opens. The stress vs. strain curve for concrete in uniaxial tensile is assumed to be linearly increasing with the strain until the crack appears, afterwards the stress to be linearly decreases and reaches zero as the concrete softens.

Bahn and Hsu (1998) carried out the parametric study and experimental test to describe the stress-strain behaviour of concrete under uniaxial compressive cyclic loading. A concrete cylinder of size 76.4 mm by 150 mm is subjected to uniaxial cyclic compressions under four different loading systems that are monotonic loading, cycles to common point, envelope curve and with random loading to investigate the parameters which dominantly control the shape of the stress-strain curve of concrete and further propose the cyclic model to simulate the behaviour of concrete under random cycles. From different loading setups, it is concluded that the unloading and reloading curves are not parallel to the initial loading curve and do not coincide too. Stiffness degradation of concrete occurs which shows the increase in the residual or plastic strain. The analaytical expressions for concrete is developed using test results to define the stress-strain relationship for concrete under cyclic axial compression. The parametric study gives out general characteristics of curve for cyclic loading such as behaviour of residual strain or unloading plastic strain, reloading strain at maximum stress and unloading and reloading curves to define the response of concrete under cyclic tests.

Lebet and Papastergiou (2016) examined the behaviour of composite beams with a new type of steel-concrete connection under cyclic loading and determines the resistance of its under cyclic loading by experimental tests. The composite action is achieved using steel-

cement grout and rough concrete cement grout at an interface of the composite girder. The shear stress which is developed at an interface between the steel and the cement grout, and at an interface between cement grout and the concrete deck mostly resist the connection to the longitudinal shear. The push-out specimen of the connection and beam test with loading up to its ultimate resistance are subjected to numerous cyclic tests to examine their behaviour under cyclic loading. In the push-out test, twelve symmetrical specimens were made-up and subjected to cyclic loading with a frequency of 1.5 Hz. The shear force is noted at certain moments by stopping the cycle to evaluate the force-slip relationship as a function of number of cycles at a loading rate of 0.25 mm/min. The cyclic loading runs up to 2 million cycles showed not any sign of failure and continued up to 5 million cycles after which it is loaded statically up to failure. The graph between residual slip obtained after removal of load and slip under peak cyclic shear load as a function of number of cycles were obtained. The residual slip and the slip at peak cyclic load were increasing with the number of cycles and stabilised after 2 million cycles. The specimens exhibit resistance to the cyclic loading, given that the peak cyclic load remains in the limit of the elastic domain. The composite beam with the new type of connection is tested with the cyclic loading up to 5 million cycles between the two load values, after which it is statically loaded up to failure. The graph between residual slip obtained after removal of load and slip under peak cyclic shear load along the composite beam as a function of number of cycles were similarly obtained here also. The graph showed that the residual slip along the composite beam and the slip at peak cyclic load in increases with cyclic loading and stabilises with the number of cycles. The composite beam is further loaded statically after 5 million of cycles up to its failure to determine its plastic resistance. The plastic resistance of the composite beam measured using rigid plastic analysis is obtained to be higher than the design plastic resistance required for such beams. Therefore, the composite beam with the new connection can resists the cyclic loading and can reach the full bending plastic resistance.

Gattesco and Giuriani (1996) discussed the behaviour of Steel and concrete composite beams with shear connectors under cyclic loading. The proposed specimens were subjected to cyclic loading between the two load values. For simulating the exact behaviour of shear connectors under reverse cyclic loading, direct shear test is performed on the proposed test specimens given in the paper in place of push-out test specimen as it does not correctly simulate the actual behaviour of the connector since the boundary conditions of the concrete parts are quite different. Cyclic tests comprise of various block of cycles, each one with different levels of maximum load on the beam. The cyclic tests have been performed by varying the shear load between the two load values and the slip increment at the end of each cycle representing the damage accumulated for each block of cycles is obtained. The minimum value of cyclic load is ranging between 30% and 10% of the peak cyclic load for each block of cycles. Each block of cycles was brought in to an end when the increment in slip showed no value or reached a constant value. The loading rate was kept constant for each cycle with a frequency of .005 Hz. The slip increment at

the end of each cycle is decreasing initially in first few cycles and then to stabilise to a constant value. It implies that a progressive damage is accumulated at each cycle. Concrete in front of embedded shear stud and in the shank of the head was damaged mostly in the initial cycles, afterwards the increment in slip tends to be constant representing progressive damage of the shank of the stud. The increment in slip increases with the load range for various block of cycles. From the cyclic tests, the slip at the end of each cycles is increases with the number of cycles and then finally becomes constant after a few initial cycles.

The given literature review helps in the developing of finite element modelling of steel concrete composite girder under cyclic loading. Zhao and Li (2008) and Zheng et al. (2009) provides assistance in developing the 3-D finite element modelling of girder which includes element type, stree-strain behaviour of concrete in compression and tension and limit of proportionality for concrete. Bi-linear stress- strain curve for steel stud and its finite element modelling has been developed from the research of Liang et al (2005). Bahn and Hsu (1998) proposed the parameters such as residual strain, reloading stress and strain which mainly dominates the behaviour of concrete subjected to cyclic loading. Lebet and Papastergiou (2016) and Gattesco and Giuriani (1996) gives the general skeloton for cyclic loading applications which includes the load values, frequency of each cycle and number of cycles and the general behaviour of the slip along the girder under cyclic loading.

2.2 Research Gap

The literature review presented above suggests the lack of methodology for numerical analysis of full-scale steel-concrete composite girder with headed shear stud connectors under cyclic loading. Lebet and Papastergiou (2016) discussed the behaviour of a new type of steel-concrete connection, not for the headed shear connectors under cyclic loading performed experimentally. Gattesco and Giuriani (1996) performed cyclic tests on the new proposed test specimens in place of push-out test to correctly simulate the actual behaviour of the connector performed experimentally. A finite element modelling technique using Abaqus is developed to simulate the behaviour of composite girder with headed shear stud under cyclic loading and the same can also be further used for the numerical validation of steel concrete composite girder subjected to cyclic tests.

2.3 Objectives

The fore mentioned research gap leads to the following objectives:

1. To develop a methodology for finite element modelling of steel-concrete composite girder with headed shear stud connectors using Abaqus under cyclic loading.
2. Numerical analysis of composite girder through parametric study which includes stress-strain behaviour of concrete and steel under cyclic loading, variation of mid-span deflection at peak loading and residual strain and stress as a function of number of cycles.
3. Behaviour of composite girder under cyclic loading as compared to if it is statically loaded up to peak cyclic load

CHAPTER 3

MATERIAL AND MODELLING

3.1 General

This chapter deals with the material properties of Concrete, Steel I-Section, Reinforcement and Headed shear studs, 3-D Finite element modelling of parts, Constraints and Interaction between them and cyclic loading behaviour and its application on simply supported Steel-Concrete Composite Girder. In this work, linear and non-linear finite element analysis of '3-D simply supported composite girder is carried out using Abaqus.

3.2 Material Properties

For the numerical analysis of the steel-concrete composite girder Abaqus requires certain material parameters which are discussed under material modelling for fore mentioned components

3.2.1 Concrete Modelling

The stress-strain behaviour of concrete under compression and tension which includes elastic and elastic-plastic behaviour of concrete has been modelled using concrete damage plasticity model.

3.2.1.1 General

In Abaqus modelling of concrete properties, it is necessary to analyze the linear and non-linear behavior of Concrete. Crack propagation is a predominant source of nonlinearity and a main culprit for ultimate failure of structures made from these materials. For Concrete Modelling, various constitutive models are proposed such as Smearing Cracking Model, Concrete Damage plasticity method, Mohr- Coulomb Plasticity, Drucker-Prager models so many more to assess non-linear behaviour of concrete. In Concrete Modelling, there is need to assess the tensile and compressive behavior of concrete under general loading. As Concrete is strong in Compression weak in tension, equation for stress strain curve is to be provided for tensile behavior and compressive behavior. The modelling of concrete must represent the behaviour of concrete before crack appears and post cracking phenomena after the crack opens. For fatigue loading and cyclic loading, degradation of modulus of elasticity takes place, 'Concrete Damage plasticity model' is generally used. The non-linear behaviour of concrete having cylindrical compressive strength 66.7 MPa having modulus of Elasticity (E_c) 36600MPa is modelled using 'Concrete Damage Plasticity Model'

3.2.1.2 Elastic behaviour of concrete

Initially Stress- Strain curve under tension and compression loading is linear up to elastic limit with its slope equals Modulus of Elasticity of Concrete (Ec). In Abaqus, A linear elastic material model having Isotropic type is taken.

$$\sigma = \varepsilon . E_c \qquad (3.1)$$

E_c is taken as 36,600 MPa and Poisson's ratio is 0.28

3.2.1.3 Concrete damage plasticity model

The concrete damaged plasticity model implemented for the material modelling of the concrete slab in ABAQUS:

1. Enables modelling of quasi-brittle material such as concrete in used for any type of elements such as solids, shells beams and trusses;
2. Makes use of the concepts of isotropic degradation of elasticity along with isotropic compressive and tensile plasticity to characterise the inelastic nature of concrete;
3. Can be implemented with reinforcement bar to model concrete reinforcement;

To fully implement CDP model in Abaqus, the following mandatory parameters should be input

Dilation Angle: The plastic volumetric strain generated during plastic shearing is controlled by the dilation angle and is assumed to be constant throughout the phenomena of plastic yielding The angle of dilation is adopted as 36° (Kmiecik and Kamiński 2011).

Eccentricity: The rate at which the function tends to be asymptotic (the flow potential approaches to be a straight line as the eccentricity is reduced to a negligible value). The default flow potential eccentricity is 0.1, which implies that dilation angle of material is unchanged over a wide range of confining stress values (Hibbitt et al. 2013).

$\mathbf{f_{b0}/f_{c0}}$ **: R**atio of 'ultimate biaxial compressive stress' to the 'ultimate uniaxial compressive stress' It is adopted as 1.16 in our analysis (Kupfer and Gerstle 1973).

$\mathbf{K_c}$ **(shape factor:** Ratio of the second stress invariant on the tensile meridian, to that on the compressive meridian, at initial yield for any given value of the pressure invariant p such that the maximum principal stress is negative, it must satisfy the condition $0.5 \leq K_c \leq 1$. The default value is (2/3) (Hibbitt et al. 2013).

Viscosity Parameter: Representation of the relaxation time of a viscoelastic system. The rate of convergence of the analysis in the softening region can be improved by using the viscoplastic alteration with a small value of the viscosity parameter (small as compared to characteristic time increment), without negotiating with the accuracy of the results. The value of viscosity parameter has been adopted as 0.00001 for the current analysis.(Hibbitt et al. 2013).

The concrete damaged plasticity model assumes that the two main failure mechanisms in concrete are the tensile cracking and the compressive crushing.

3.2.1.3.1 Numerical model for compressive behaviour

In the compressive behaviour of concrete, the stress–strain equation suggested by Carreira and Chu (1985) has been employed to model the elastic–plastic material characteristics with strain softening (Carreira and Chu 1985).

$$\frac{f_c}{f'_c} = \frac{\beta\left(\frac{\varepsilon}{\varepsilon'_c}\right)}{\beta - 1 + \left(\frac{\varepsilon}{\varepsilon'_c}\right)^{\beta}} \quad (3.2)$$

and

$$\beta = \frac{1}{1 - \frac{f'_c}{\varepsilon'_c \, Ec}} \quad (3.3)$$

For $\beta \geq 1.0$ and $\varepsilon \leq \varepsilon_u$

f'_c is the maximum stress usually considered as the concrete strength and determined in accordance with ASTM C 39, "Standard Test Method for Compressive strength of Cylindrical Specimens" (Boyer 1987).

ε'_c is the strain corresponding with the maximum stress.

$$\varepsilon'_c = (0.71 * f'_c + 168) * 10^{-5} \quad (3.4)$$

β is a material parameter that depends on the shape of the stress-strain curve.
f_c is the compressive stress corresponding to the compressive strain ε.

The stress-strain graph obtained for f'_c is obtained as given below

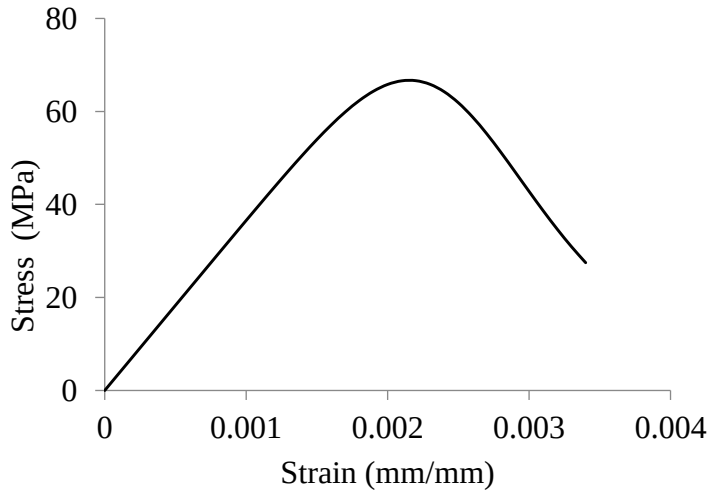

Figure 3.1 Actual stress-strain graph for concrete in compression (Carreira and Chu 1985)

In the Concrete Damage Plasticity , there is need to idealize the stress- strain behaviour of concrete in compression for the development of a proper damage simulation model for the analysis of reinforced concrete deck slab under static and dynamic loading (Hibbitt et al. 2013). In the numerical modelling of concrete behaviour 0.3 f′c is usually proposed as the limit of elasticity. (Chen 1988). Beyond this limit the concrete material loses strength quickly. To define the stress-strain relationship, there is need to enter stress (f_c), inelastic strain (ε_{ie}) corresponding to stress values, and damage properties (d_c). Further a corrective measure should be taken to ensure that the plastic strain values (ε_p) are neither negative nor decreasing with increased stresses (Wahalathantri et al. 2011) .

$$\varepsilon_{ie} = \varepsilon - \varepsilon_e \quad (3.5)$$

ε_e is the compressive strain corresponding to linear of elasticity i.e. 0.3 f'_c

$$d_c = \frac{\varepsilon_{ie}}{\varepsilon} \quad (3.6)$$

and

$$\varepsilon_p = \varepsilon_{ie} - \frac{dc}{1 - dc}\varepsilon_e \quad (3.7)$$

So, the idealized stress-strain graph for concrete in compression is given below.

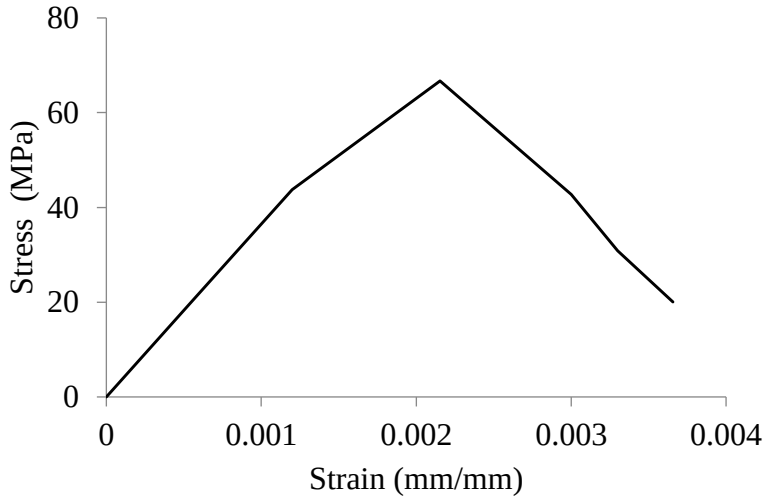

Figure 3.2 Idealized stress-strain graph for concrete in compression

3.2.1.3.2 Numerical model for tensile behaviour

Under the behaviour of uniaxial tension, the stress vs. strain of concrete can be idealised as a line originating from origin reaching up to a value of maximum tensile stress corresponding to the generation of the first crack due to the magnification of microcrack present in the interfacial transition zone of concrete. The generation of microcracks is

represented macroscopically when the stress is increased beyond the failure stress representing the strain softening phenomena in concrete. The concrete under uniaxial tension is modelled using the stress vs. strain curve created by the equations suggested by Carreira and Chu (1986) to represent its elastoplastic material characteristics(Carreira and Chu 1986).

$$\frac{f_t}{f'_t} = \frac{\beta\left(\frac{\varepsilon}{\varepsilon'_t}\right)}{\beta - 1 + \left(\frac{\varepsilon}{\varepsilon'_t}\right)^{\beta}} \qquad (3.8)$$

- β is a parameter that depends on shape of the stress vs. strain diagram, taken as same of concrete in compression.
- f'_t is the maximum stress usually taken as the $0.623\ (f'_c)^{0.5}$ (Committee et al. 2008)
- ε'_t is the strain corresponding with the maximum stress, adopted as $0.1*\varepsilon'_c$.
- f_t is the tensile stress corresponding to the tensile strain ε.

The stress-strain graph obtained for f'_c is obtained as given below.

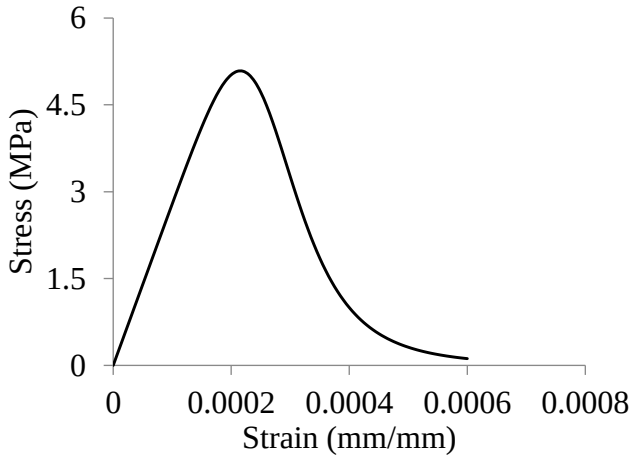

Figure 3.3 Actual graph of reinforced concrete stress vs strain curve in tension

In the numerical modelling of concrete behaviour $0.6\ f'_t$ is usually proposed as the limit of elasticity. (Chen 1988). Beyond this limit the concrete material loses strength quickly. To define the stress-strain relationship, there is need to enter stress (f_c), inelastic strain (ε_{ie}) corresponding to stress values, and damage properties (d_t). Further a corrective measure should be taken to ensure that the plastic strain values (ε_p) are neither negative nor decreasing with increased stresses (Wahalathantri et al. 2011)

$$\varepsilon_{ie} = \varepsilon - \varepsilon_e \qquad (3.9)$$

ε_e is the compressive strain corresponding to linear of elasticity i.e. 0.6 $f'_{t.}$

$$d_t = \frac{\varepsilon_{ie}}{\varepsilon} \quad (3.10)$$

and

$$\varepsilon_p = \varepsilon_{ie} - \frac{d_t}{1-d_t}\varepsilon_e \quad (3.11)$$

So, the idealized stress-strain graph for concrete in tension is given below.

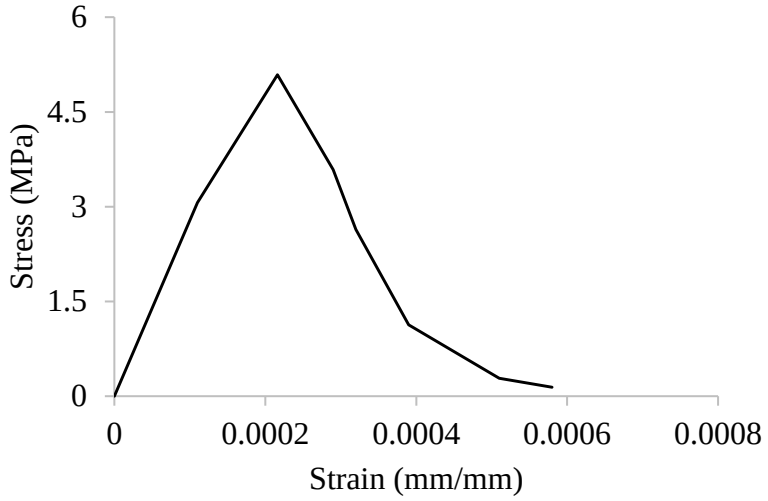

Figure 3.4 Idealized stress-strain graph for concrete in tension

3.2.2 Steel modelling

The details of steel used in the modelling of the full-scale steel concrete girder is summarised in the following table:

Table 3.1 Details of steel used in composite girder

Part	Yield Limit (MPa)	Ultimate Strength (MPa)	Poisson's Ratio	Modulus of Elasticity (MPa)
Structural Steel	413	574.8	0.3	200000
Reinforcement	580	669.773	0.28	200000
Headed Shear Stud	321.98	492.05	0.28	166488

3.2.2.1 Elastic behaviour of steel

Initially Stress- Strain curve under tension and compression loading is linear up to elastic limit with its slope equals Modulus of Elasticity of Steel (E_s). In Abaqus, A linear elastic material model having Isotropic type is taken.

$$\sigma = \varepsilon . E_s \quad (3.12)$$

3.2.2.2 Plastic behaviour of steel

A kinematic/isotropic hardening model is implemented in Abaqus to account for the non-linear plastic behaviour of steel such as strain hardening, Bauschinger effect.

3.2.2.2.1 Isotropic hardening of steel

For isotropic hardening, if a solid is deformed plastically, then unloaded and reloaded, an increase in stress required for yielding is observed as compared to that of in the first cycle. Such behaviour continues as long as the specimen reloaded beyond its maximum stress subjected during the previous cycle till the solid deforms plastically. Basically, isotropic hardening represents the behaviour in which, if the specimen is loaded in tension beyond the yield point, unloaded, then again loaded it in compression, yield will only be observed when it is loaded in beyond the maximum load reached in tension. Alternatively, isotropic hardening can be explained as the same amount of increase in yield stress of compression with the increase in the yield stress under tension due to hardening even though the solid might not have been subjected to the compressive load. Plasticity of ductile material can be implemented using this is a type of hardening used in material models for finite element analysis. Although, Isotropic hardening model cannot be used to accurately represent plasticity of real materials as it does not account for Bauschinger effect and accurate hardening of materials after few cycles

3.2.2.2.2 Kinematic hardening of steel

The kinematic hardening models generally used to implement the behaviour of ductile materials subjected to reversed cyclic loading are independent of equivalent pressure stresses. These models can be successfully used to describe the plastic behaviour

of the most of the metals subjected to cyclic loading, except voided metals (Hibbitt et al. 2013). The kinematic hardening models:

- Can be used to implement the inelastic behaviour of materials under the effect of cyclic loading;
- Can be used for modelling of linear kinematic hardening and nonlinear kinematic/isoptropic hardening;
- Also incorporates for multiple backstresses in kinematic/isotropic hardening
- Can be implemented in any analysis where elements with displacement degree of freedom are used;
- Can be applied to models where yield is dependent on rate of loading;
- Can be used in conjunction with swelling and creep; and
- Define the elastic behaviour of the structure with the help of linear elasticity model for metals.

In order to implement above mentioned hardening model stress vs strain data for structural steel under tension is required to input. Stress vs strain curve for structural steel, reinforcements are obtained from Atlas of stress-strain curves" second edition ASM International "The Material Information Society(Boyer 1987) whereas stress vs strain curve for headed shear studs are obtained from experimental results available in literature (Kumar et al. 2017). The hardening region of curve for structural steel and reinforcement is approximated using a trilinear curve.

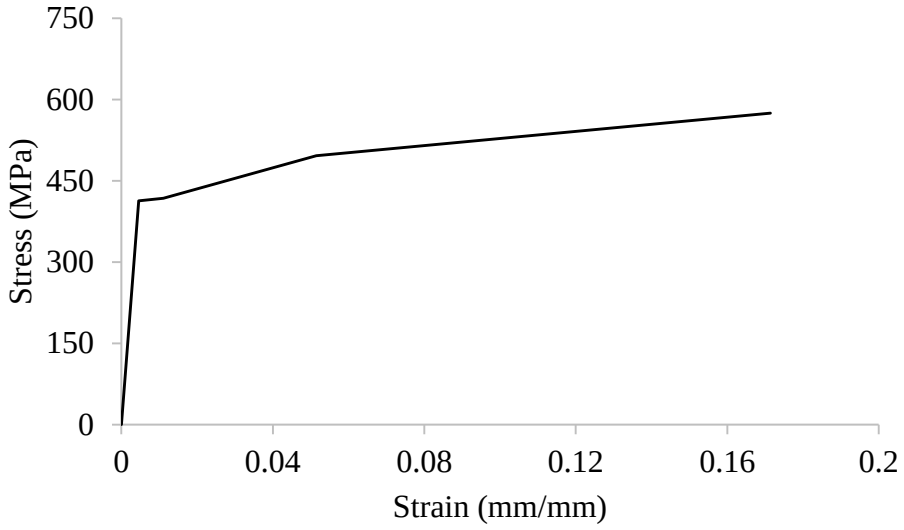

Figure 3.5 Stress-strain graph for structural steel

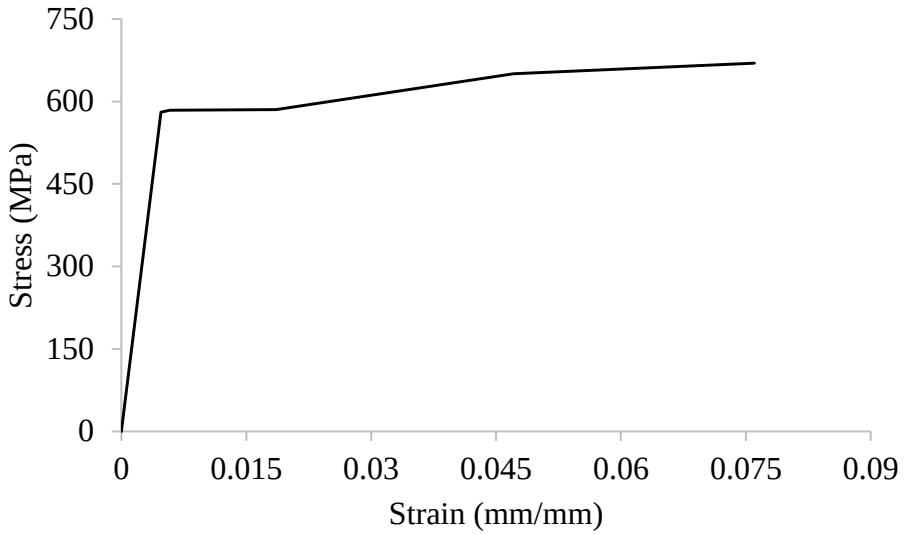

Figure 3.6 Stress-strain graph for reinforcement steel

The material properties for headed shear studs obtained experimentally having young's modulus of stud is taken as 166.488 GPa and poison's ratio is taken as 0.28. The Bi linear curve is adopted for the non-linear material properties in Abaqus 6.13.

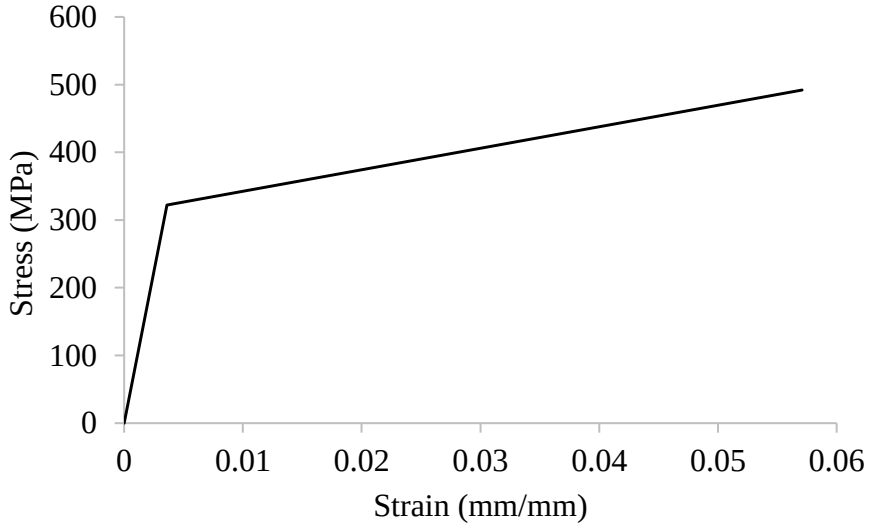

Figure 3.7 Stress-strain graph for headed shear stud

3.3 Structural Modelling

The physical implementation of the dimensions, shape, boundary conditions, assembly of the components, constraint between these structural components of the representative structure are required in Abaqus in order to perform analysis of the representative structure. A general overview of the representative structure, physical modelling, 3D finite element meshing techniques are discussed under the structural modelling of the steel concrete composite girder.

3.3.1 General overview of representative structure

The representative steel-concrete composite girder consists of a concrete slab (800mm × 140mm), unsymmetrical I steel section having top flange width as 140mm and bottom flange width equals 200mm connected together by headed shear studs of diameter 19 mm and a height of 114 mm. Twenty-four pairs of headed studs were used in the composite plate girder with a uniform longitudinal spacing of 366.591mm and a transverse spacing of 76 mm. Concrete slab is provided with transverse reinforcement in the form of shear stirrups of 10 mm diameter bar with spacing of 180 mm centre to centre and a cover of 20 mm, 12 number of 12 mm diameter bar as longitudinal reinforcements. The composite girder is supported on simple supports with an effective span of 8.5 m.

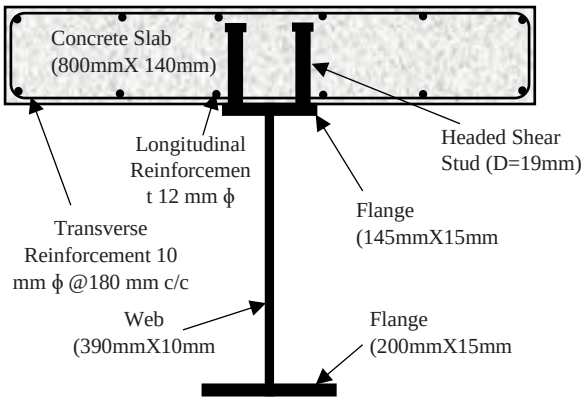

Figure 3.8 Section X-X of steel-concrete composite girder

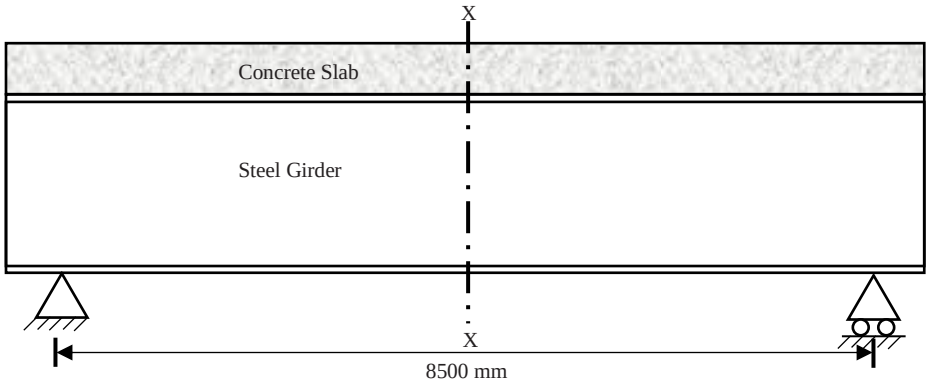

Figure 3.9 Longitudinal view of composite girder

3.3.2 Finite element modelling of components

Shape, dimensions and type of elements are required to input in Abaqus using certain modelling techniques. Implementation of such techniques is explicated under finite element modelling of components. In order to obtain accurate results from the finite element analysis, all the composite plate girder components must be properly modelled. The composite plate girder components comprise the steel plate girder, concrete slab, headed stud, and reinforcement bars.

3.3.2.1 Concrete slab

A solid 3D type deformable concrete slab has been created using extrusion feature available in Abaqus. For meshing Abaqus provides a wide range of elements for different geometries and analysis types. For meshing of the concrete slab linear hexahedron type C3D8R (8-node trilinear brick) element is used, where R stands for reduced integration. Reduced-order integration (primarily used by Abaqus/Standard) allow for fast and cheap calculation of the element matrices but may have significant effect on the accuracy of the element for a given problem.

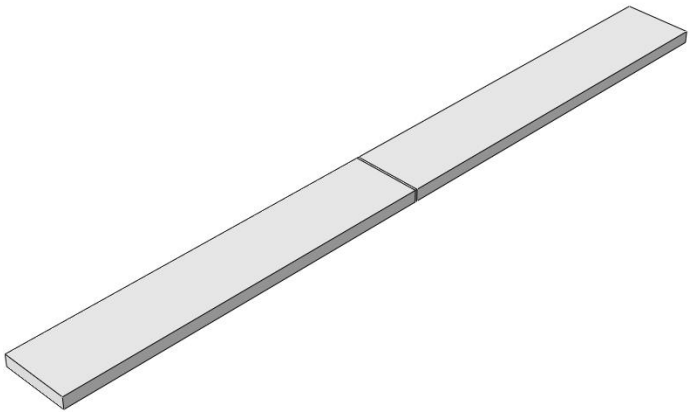

Figure 3.10 Solid 3-D view of concrete slab

3.3.2.2 I-Section

A solid 3D type deformable I-section is created using extrusion feature available in ABAQUS, by sketching a profile of the same. Web and flange portions are partitioned and separated by cuts using datum plane to ensure uniform mesh size and connectivity. For meshing of I-Section linear hexahedron type C3D8R (8-node trilinear brick) element with approximate mesh size equals 33 mm generating 40808 total number of elements. Shear studs are assigned Properties of it while I-section structural steel member is assigned properties of it.

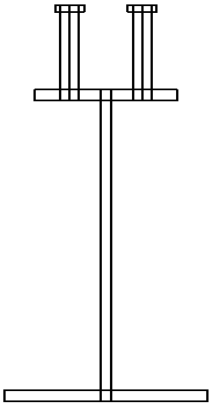

Figure 3.11 Partitioned I-section along with shear studs

3.3.2.3 Headed Shear Stud Connectors

Headed shear connectors were sketched and extruded over the top flange surface of I-section. This method of extrusion eliminates the need of tie constraint between the I-section and studs. Shear studs are difficult to mesh. Circular geometry of shear studs leads to the creation of improperly proportioned elements during meshing. To overcome this problem two diametric cuts are applied on studs, along with a small circular cut which is extruded over the full length of stud. While partitioning the studs in conjunction with the I-section all the cuts are extended into the flange and additional cuts are applied to separate interface of studs and flange in the form of a square. An additional circular cut equal to the leg diameter of stud is applied. All the cuts applied to the studs are continued in the I-section to avoid discontinuity at the interface of stud and flange of I-section which may lead to poor meshing at their interface. The large number of shear connectors distributed over the flange of makes it difficult to apply the required cuts for each stud individually due to its repetitive nature. To solve this difficulty, required cuts has been automated using python scripting feature of Abaqus. The shear studs are also meshed using linear hexahedron type C3D8R (8-node trilinear brick) element.

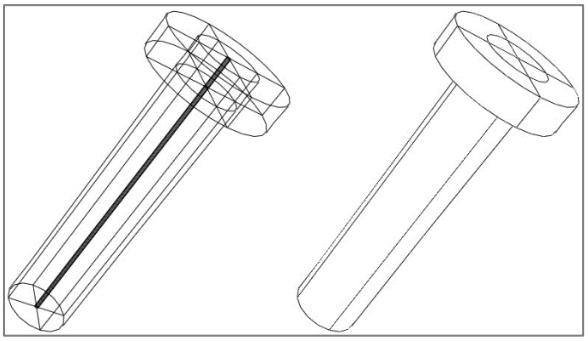

Figure 3.12 A wireframe and a solid view of shear stud with cuts

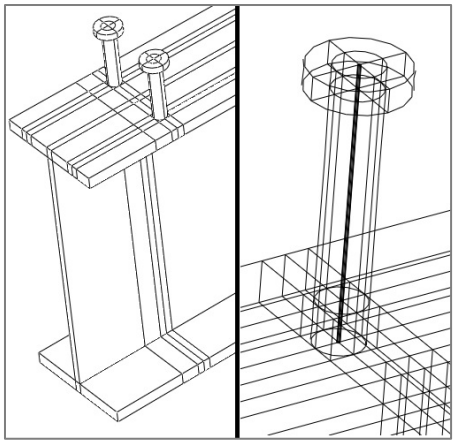

Figure 3.13 A view of extended cuts of studs into the I-section

3.3.2.4 Reinforcement

Reinforcement (both Transverse and Longitudinal) are created using 3D deformable wire shape. As variation of stresses and displacements are not required in the cross section of the rebars, wire shape elements are computationally efficient.

3.3.3 Constraints between modelled parts

Embedded region constraint is provided which helps in partially or fully eliminate degrees of freedom of a group of nodes and couple their motion to the motion of a master node (or nodes). Structural I-Section comprising of twenty-four pairs of headed shear stud connectors and reinforcement act as embedded region embedded into concrete girder acts as host region.

3.3.4 Boundary conditions, loading and analysis

Boundary conditions and its nature and magnitude of the applied load are so adjusted that they represent the real time supports and loads over the structure. Techniques to implement the supports and loads over the structure are explained under this section.

3.3.4.1 Boundary conditions

In order to apply boundary conditions of simple supports the composite girder is extended by 90 mm in both direction, so that horizontal slip of the girder over the roller of the simple support does not result in the collapse of structure. Hinged end of simple support is modelled by restricting only displacements in all three directions i.e. (U_x=U_y=U_z=0) on a line at the bottom of the flange of I-section at one end. Whereas roller support is modelled by restricting displacement only in vertical and transverse directions i.e. (U_x=U_y=0) on a line at the bottom of the flange of I-section at another end of the girder.

3.3.4.2 Loading and analysis

The composite girder is loaded with static load theoretically found from the rigid plastic analysis, to find its yield and collapse load, along with different parameters such as central deflection of the girder, stress and strain at the bottom of the flange of I-section and on the top of concrete at the mid span, support reactions. The analysis of the girder under the static load performed using Abaqus/Standard to establish a control for the comparison of desired parameters with that of the girder under the cyclic load. All the loads are applied at the mid span at the top of the concrete slab over an area of 800 mm × 24mm. For the cyclic tests, a vertical cyclic load of sinusoidal nature with no reversal loading at a frequency of 2Hz (time period of one cycle is 0.5 sec) is applied at the mid span of the composite beam on the loaded surface. As Cyclic loading represents variation of load with time (or frequency), amplitude curve is to be given which is variation of relative load with time (or frequency) throughout the analysis in the tabular form in Abaqus 6.13. Amplitude Curve for different number of cycle is obtained using equations given below

$$A_t = A_0 \sin 2\pi t \qquad (3.13)$$

$A_0 = 1$

A_t represents amplitude at any time 't', varies from 0 to 1.

A_0 is the peak amplitude whose value is 1.

$$L_t = L_0 \times A_t \qquad (3.14)$$

L_0 is the peak load at peak amplitude.

L_t represents load at any time 't' varies from 0 to L_0.

For analysis of composite girder under cyclic loading, peak load is applied whose value is between the yield load and collapse load to account for non-linear behaviour of steel and concrete to be taken as 450 kN.

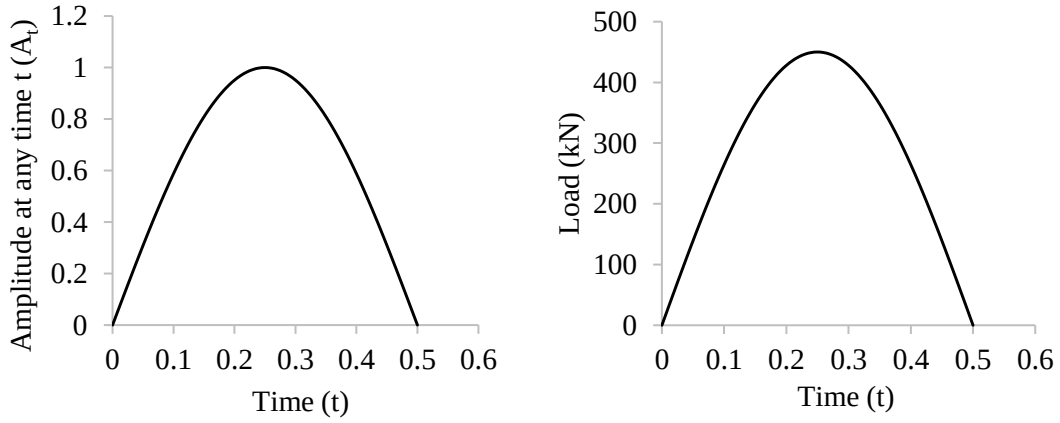

Figure 3.14 Amplitude curve and Load curve for one cycle

Behaviour of Composite Girder under cyclic loading for 25 cycles and 100 cycles is compared with if it is statically loaded up to the peak cyclic load. For numerical analysis of composite girder under cyclic loading static general analysis is performed for two cases of cycles i.e. 25 cycles and 100 cycles and certain parameters such as mid-span deflection of composite girder at peak cyclic load, residual stress and strain obtained after removal of load in cyclic loading at bottom of the steel section and at the top of the concrete slab along the composite girder, longitudinal stress and strain at peak loading at the bottom of the steel and at the top of the concrete, reaction at the supports and stress-strain graph for concrete and steel for 25 number of cycles and 100 number of cycles are plotted and compared.

CHAPTER 4

NUMERICAL VALIDATION

4.1 General

Numerical validation is necessary for the development of finite element modelling technique to carry out the linear and non-linear analysis of steel and concrete structures. In this work, Abaqus 6.13 Standard is used to carried out steel and concrete behaviour under static and dynamic loading situations. For the validation of steel and concrete properties two finite element models have been developed in Abaqus 6.13 Standard and its analysis is carried out to simulates its behaviour with the original studies. The one is Gable frame consisting entirely of steel to validate the steel properties (Vogel 1985) and another one is Steel-concrete composite girders (Mans, Yakel et al. 2001) to validate concrete properties. The results of all the models have been compared with the previous studies to verify the finite element modelling technique and material properties.

4.2 Numerical Validation of Steel Modelling

In this paper, linear and non-linear finite element analysis of gable portal frame pinned support is conducted for verifying the reliability and accuracy of the elastic-plastic analysis by ABAQUS software. The gable frame has been modelled for finite element analysis (FEA) analysis with appropriate modeling of element size and mesh. Material Steel is used for elastic and plastic analysis. For plastic analysis stress- strain curve data of A36 high-strength steel is used, and a tri-linear plastic curve is used. For modelling Section IPE 360 is used, dimensions are w_f = 170 mm, t_f = 12.7 mm, t_w = 8 mm, h = 360 mm. Web and flange portions are partitioned and separated to ensure uniform mesh size and connectivity.

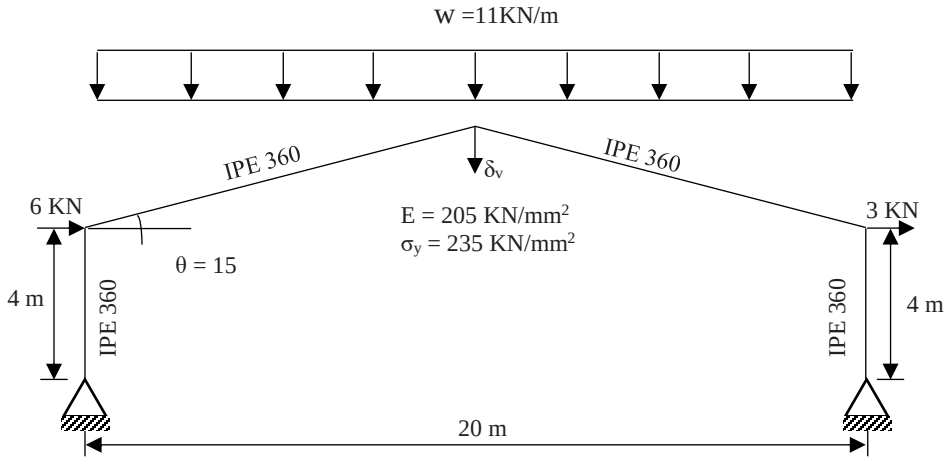

Figure 4.1 Schematic diagram of gable frame arrangement (Vogel 1985)

For analysis the lateral load displacement at right knee joint for various loads factors by Abaqus software is obtained and the Load factor vs. Horizontal deformation curve is plotted and compared with the plastic hinge analysis of paper.

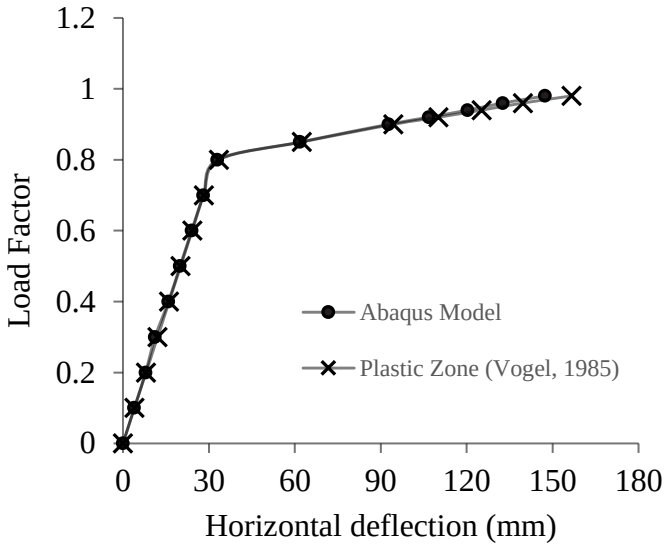

Figure 4.2 Load Factor Vs Horizontal deflection

From the graph the Horizontal deformation obtained from the analysis by Abaqus is found to be in close agreement with deflection from Vogel 1985.

4.3 Numerical Validation of Concrete Modelling

In this work, linear and non-linear finite element analysis of '3-D simply supported composite steel plate girder tested by model is carried out using Abaqus for validation of concrete and steel properties. The composite plate girder tested by (Mans et al. 2001) was modelled in this work using ABAQUS. In order to obtain accurate results from the finite element analysis, all the composite plate girder components must be properly modelled.

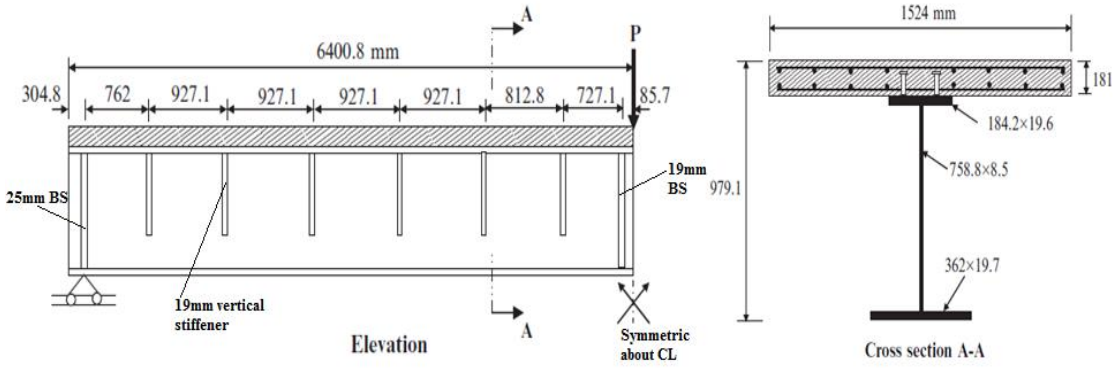

Figure 4.3 Longitudinal and cross-sectional view of steel-concrete composite girder

The non-linear behaviour of concrete having cylindrical compressive strength 30.5MPa is modelled using 'Concrete Damage Plasticity Model', uses concepts of isotropic damaged elasticity in combination with isotropic tensile and compressive plasticity to represent the inelastic behaviour of concrete. In the concrete compression and tension, the

stress–strain equation suggested by Carreira and Chu (1985) has been employed to model the elastic plastic material characteristics.

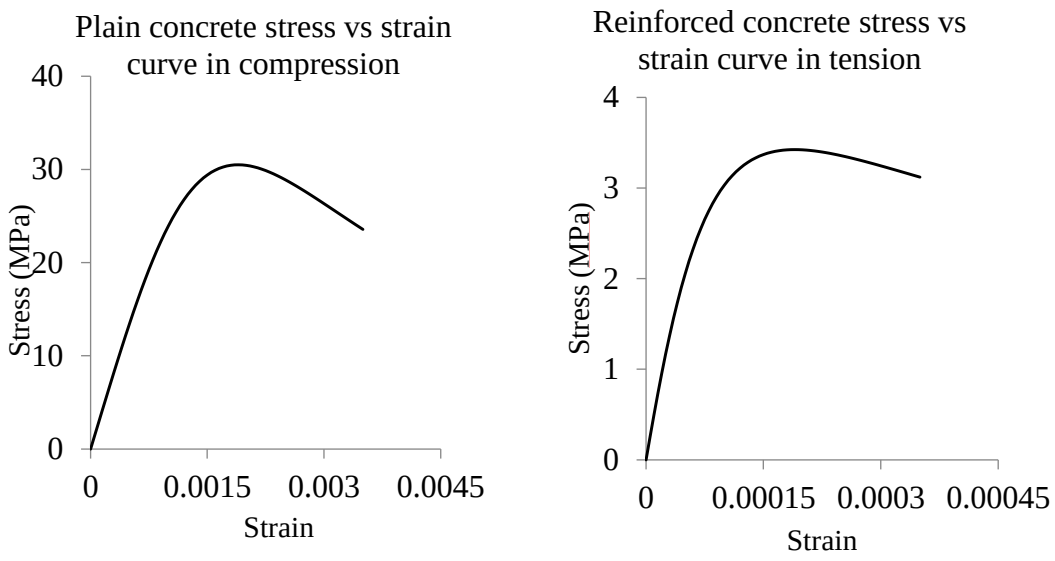

Figure 4.4 Stress-Strain curve of concrete in compression and tension

For Structural Steel Properties in analysis steel with yield stress 551 MPa and ultimate stress 721 MPa is used. For plastic analysis. The curve is idealised as a trilinear curve. The concrete slab had reinforcement steel bars, having a yield stress of 413 MPa. Eighty pairs of headed studs were used and the bilinear curve is adopted for the non-linear material properties in Abaqus. For modelling and meshing of concrete, a solid 3D type deformable concrete slab is created using extrusion feature available in Abaqus.

For Analysis and Validation of concrete properties, a load vs. midspan deflection curve predicted experimentally and numerically in Abaqus was compared as shown in the following chart.

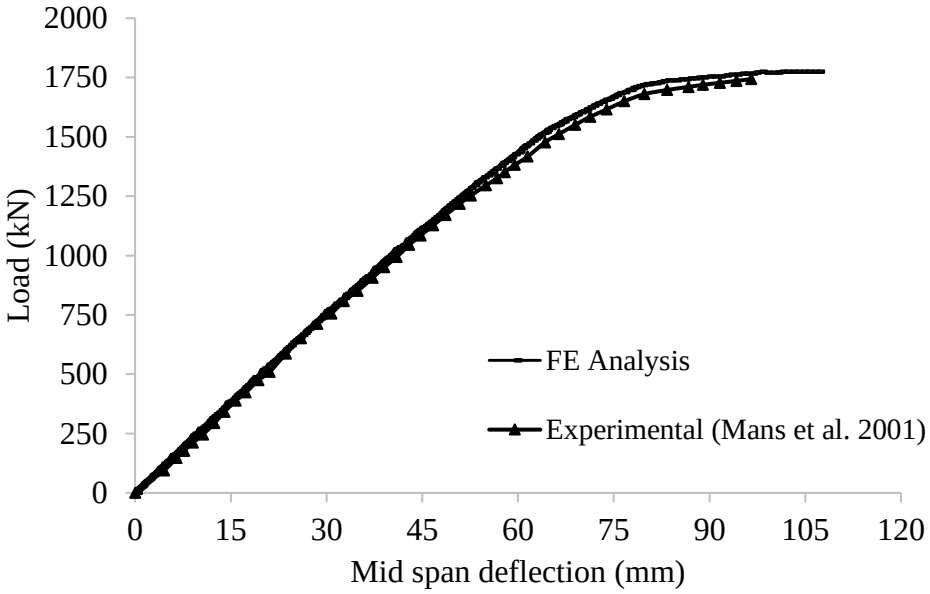

Figure 4.5 Comparison of load vs mid-span deflection graph by FE analysis and experimental results

It can be shown that generally good agreement was achieved between experimental and numerical relationships. From the above curve, it can be concluded the material properties used for composite girder are closely resembling the actual material properties and hence these properties can be used for further analysis.

CHAPTER 5

RESULTS AND DISCUSSION

5.1 Static Analysis

From the theoretical rigid plastic analysis of Steel-Concrete composite girder, ultimate load is found to be 576.91 KN. The composite girder is loaded with ultimate load theoretically found from the rigid plastic analysis at the mid span at the top of the concrete slab over an area of 800 mm × 24mm to find its actual yield and ultimate load. The actual yield and ultimate load are found to be 424.57 kN and 505.6152 kN which is in close agreement with the theoretically yield and ultimate load. The lowered actual ultimate load may be because the cross section of composite girder is not reaching its full plastic moment carrying capacity (Mp) as assumed in theoretical rigid plastic analysis of composite girder.

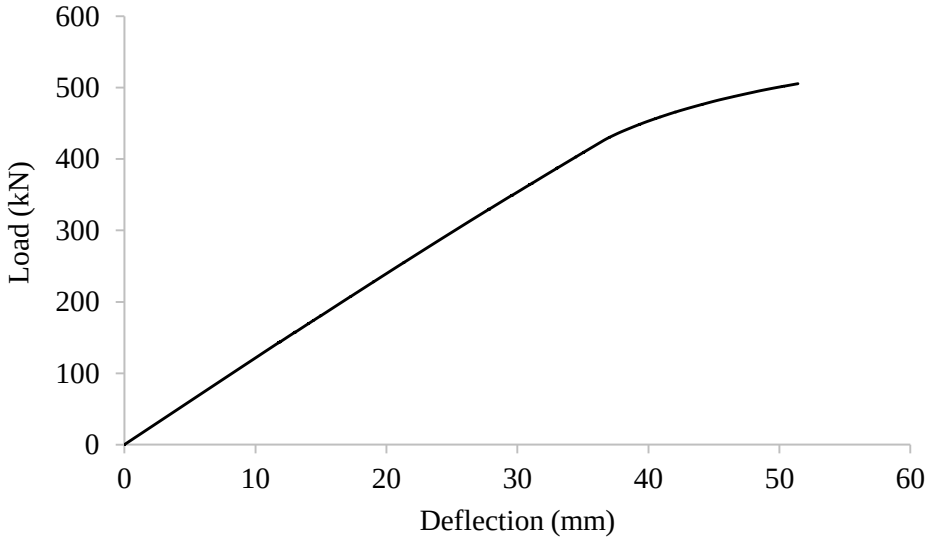

Figure 5.1 Load vs Mid-span deflection of composite girder

The mid-span deflection of the simply supported composite girder at ultimate load is found to be 51.418 mm.

The stress-strain curve for steel section at the bottom, mid-span of the composite girder under static loading is given below. As the applied loading exceeds its actual yield load i.e. 424.57 kN the stress strain curve shows yielding of the steel at the bottom of the flange due to increase in longitudinal stress of steel beyond its yield limit.

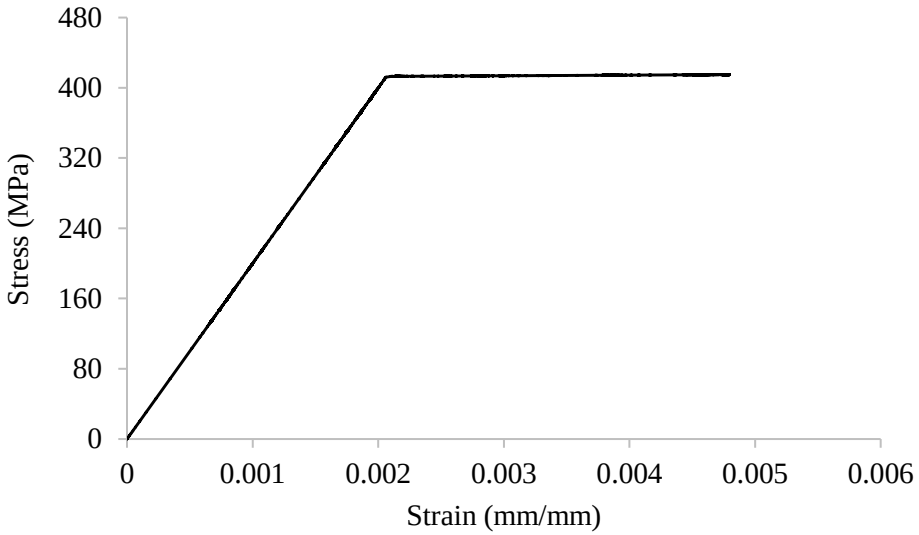

Figure 5.2 Stress vs. Strain curve at mid-span of the bottom of steel flange

Concrete slab under point loading acts in compression and the longitudinal stress and strain increases as the loading increases. The longitudinal stress at mid-span of the top of concrete slab is found to be 42.94 MPa at failure. The stress vs. strain curve for concrete in static analysis is given below.

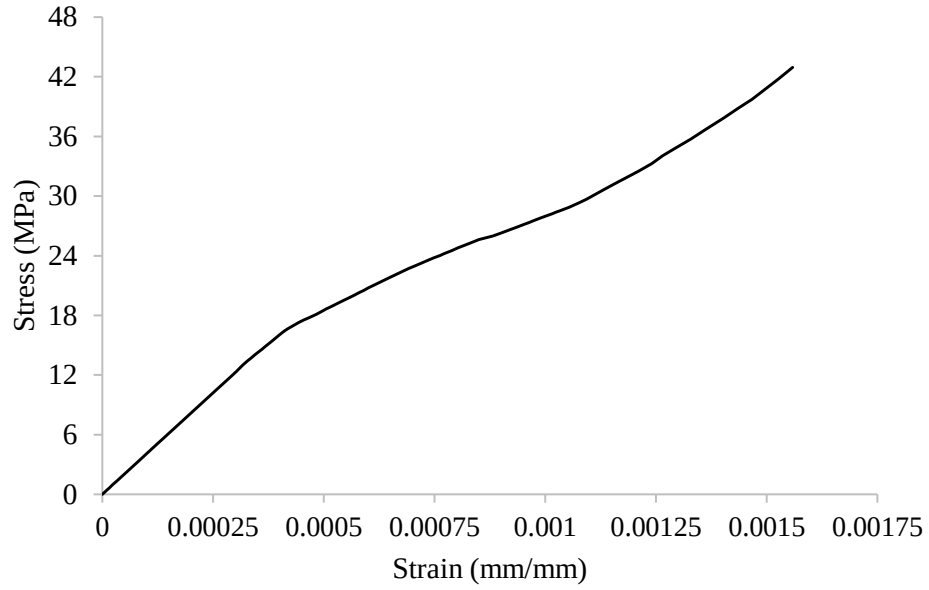

Figure 5.3 Stress Vs. Strain curve for concrete in static analysis

For the behaviour of composite girder under cyclic loading, Peak Load (L_0) which is to be adopted between yield load i.e.429.239 kN to account for non-linear behaviour of materials and ultimate load for collapse i.e. 505.61 kN is obtained as 450 kN. The given table below shows the certain parameters value at ultimate load and at load in static analysis equivalent to peak cyclic load (L_0) which may help in the comparison of behaviour of composite girder under cyclic loading with static loading.

Table 5.1 Parameters at ultimate load and peak cyclic load under static analysis

S.N.	Parameters	At Peak cyclic load (L_0)	At ultimate load
1.	Mid-span deflection of Composite Girder	39.5 mm	51.41 mm
2.	Longitudinal stress at mid-span top of concrete slab	31.17 MPa (Compressive)	42.94 MPa (Compressive)
3.	Longitudinal strain at mid-span top of concrete slab	-0.00115 (Compressive)	-0.00156 (Compressive)
4.	Longitudinal stress at mid-span bottom of steel slab	413.74 MPa (Tensile)	415.09 MPa (Tensile)
5.	Longitudinal strain at mid-span bottom of steel slab	0.00256 (Tensile)	0.004796 (Tensile)
6.	Reaction at pinned support	225 kN	252.6 kN

5.2 Numerical analysis for 25 number of cycles

In the numerical analysis of composite girder under cyclic loading, static general analysis is performed for which Peak Load (L_0) is applied as 450 kN for 25 number of cycles. The time period of each cycle is 0.5 sec thus total time period for 25 cycles will be 12.5sec. The various parameters such as mid-span deflection of composite girder at peak loading and after removal of load in cyclic loading i.e. residual deflection, residual strain at bottom of the steel section and at the top of the concrete slab, longitudinal stress at peak loading and strain at the bottom of the steel and at the top of the concrete along the composite girder, reaction at the supports and stress-strain graph for 25cycles are plotted and compared.

The mid-span deflection of the composite girder at peak loading for 25 number of cycles is given below.

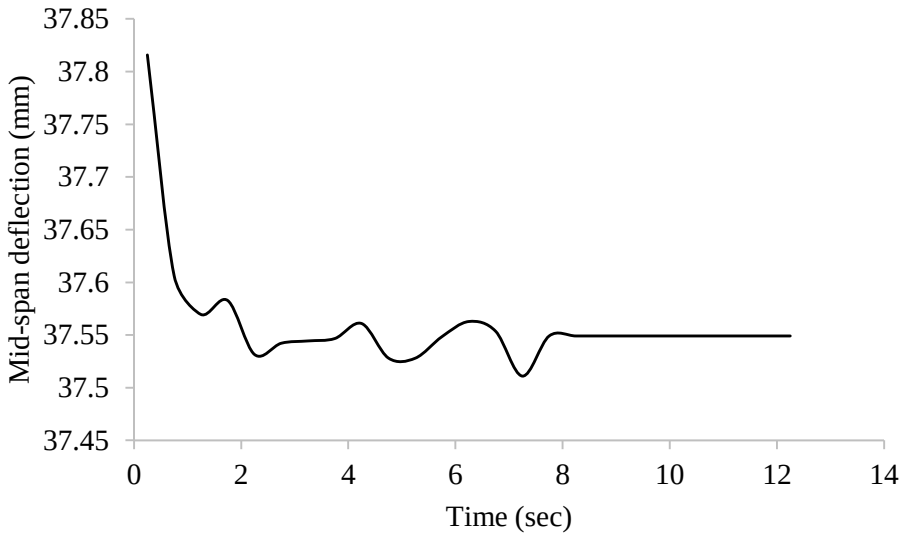

Figure 5.4 Variation of mid-span deflection of composite girder at peak loading for 25 cycles

From graph, it can be shown that initially mid-span deflection of the composite girder is more but as the cycles increases mid-span deflection decreases and finally become constant at 37.55 mm which is lower than the mid-span deflection at peak cyclic load i.e.39.5 mm found during static analysis. This behaviour may be due to increase in residual deflection of the composite girder when loading reaches zero under cyclic loading.

The mid-span deflection of the simply supported composite girder after removal of load in 25 number of cycles i.e. residual deflection is given below.

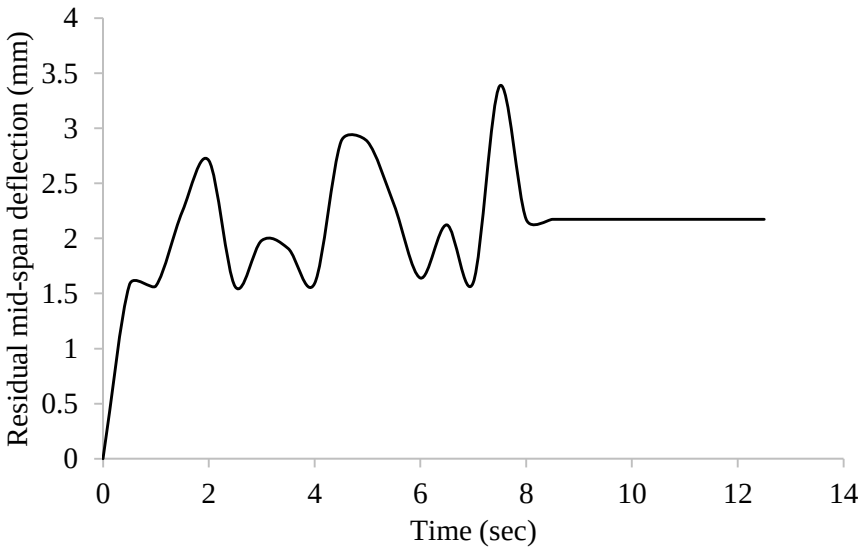

Figure 5.5 Variation of residual mid-span deflection of composite girder for 25 cycles

From the graph, it is clearly shown that residual deflection increases as the number of cycles increases and it became finally constant at 2.17 mm.

The longitudinal stresses at the mid-span bottom of the steel flanges for 25 number of cycles is given below and it can be shown that that it is cyclic in nature.

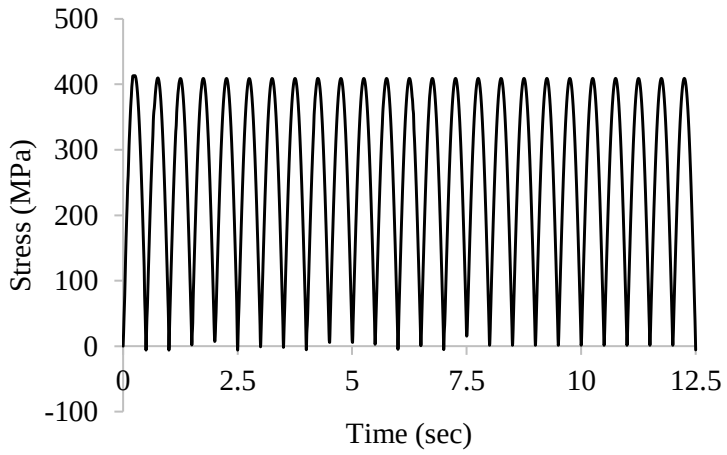

Figure 5.6 Stress at mid-span bottom of steel flange for 25 number of cycles

The longitudinal stresses at the mid-span bottom of the steel flanges and at the mid-span top of the concrete slab during peak loading are shown below.

From the graph, for steel it is clearly shown that longitudinal stresses decrease as the number of cycle increases and finally become constant at 409 MPa which is lower than the longitudinal stress at peak cyclic load i.e. 413.74 MPa found during static analysis whereas for concrete longitudinal stresses increase as the number of cycle increases and finally become constant at 40 MPa which is more than the longitudinal stress at peak cyclic load i.e. 31.17 MPa found during static analysis.

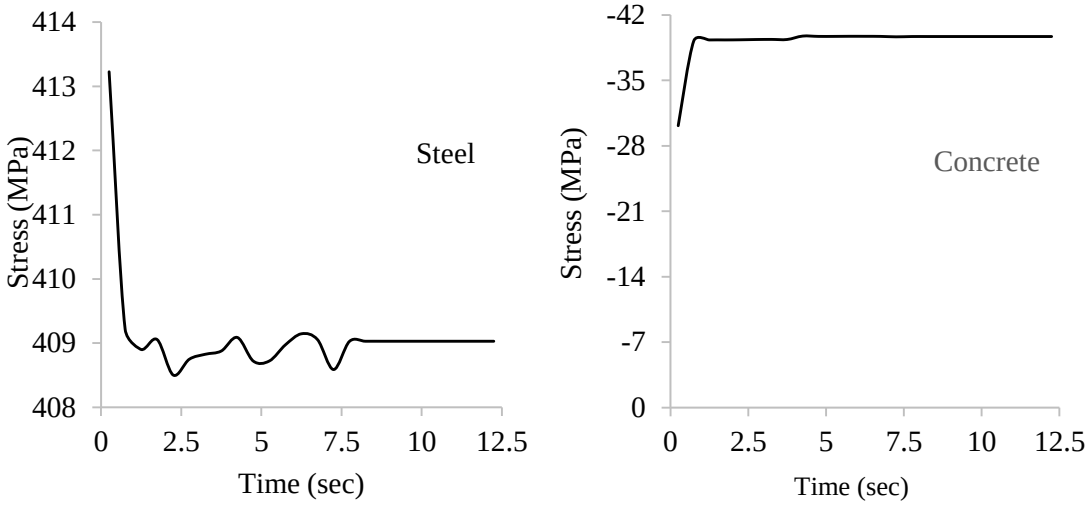

Figure 5.7 Variation of stress for steel and concrete at peak loading for 25 cycles

The longitudinal stresses at mid-span bottom of the steel flanges and at mid-span top of the concrete slab after removal of load in 25 no. of cycles i.e. residual stress are shown below.

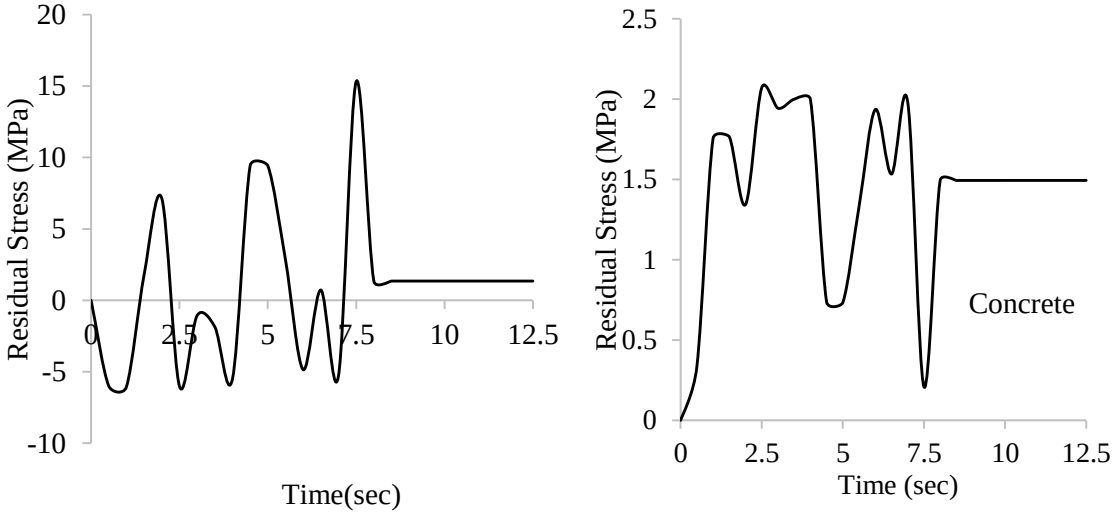

Figure 5.8 Variation of residual stress for steel and concrete for 25 cycles

From the graph, for steel it is shown that residual stress increases as the number of cycles increases and finally becomes constant at 1.35 MPa. For concrete residual stress are tensile in nature, increases as the number of cycle and finally become constant at 1.49 MPa.

The longitudinal strain during peak loading and the longitudinal strain during unloading for 25 number of cycles i.e. residual strain at mid-span bottom of the steel flange graphs are shown below. From the graph, it is clearly shown that longitudinal strain at peak loading decreases as the number of cycle increases and finally become constant at 0.00237 which is lower than the longitudinal strain at peak cyclic load i.e. 0.00256 found during static analysis.

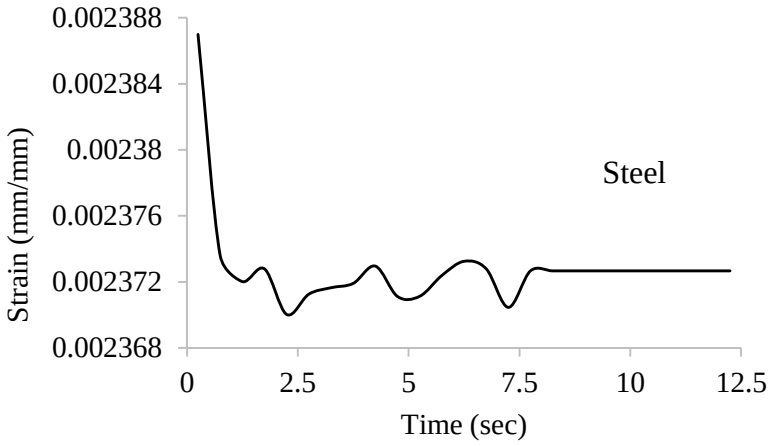

Figure 5.9 Variation of strain for steel at peak loading for 25 cycles

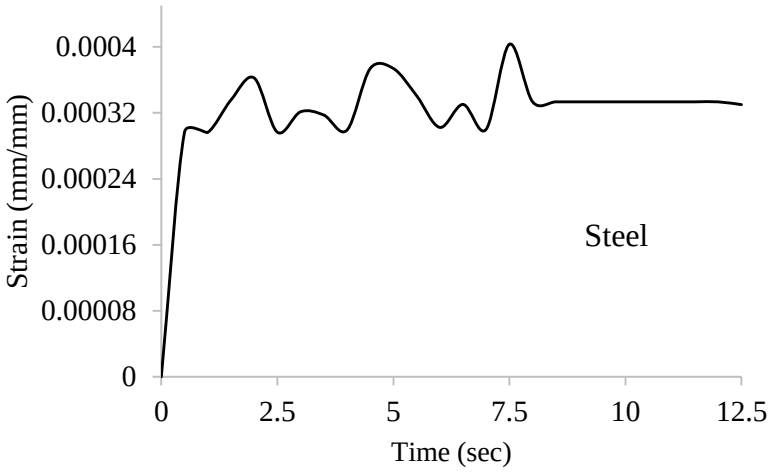

Figure 5.10 Variation of residual strain for steel for 25 cycles

From the graph, it is shown that the residual strain increases as the number of cycles increases and finally become constant at 0.00033.

The stress vs. strain graph at the mid-span bottom of the steel flange for 25 numbers of cycle is given below.

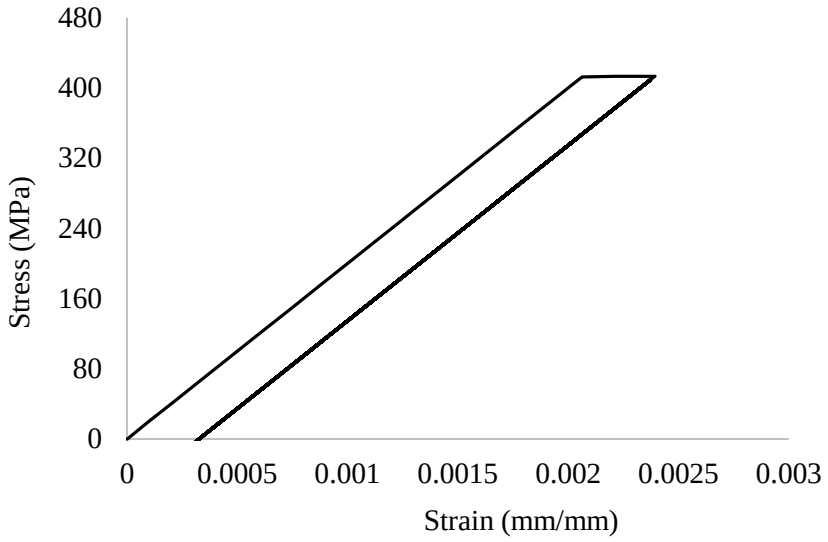

Figure 5.11 Stress vs. Strain graph of steel for 25 number of cycles

This behaviour of stress-strain graph under cyclic loading may be due to plastic shakedown phenomena (Hassan and Kyriakides 1992). In the consideration of elastic-mechanic components subject to uniaxial cyclic applied loads, if the load never induces plastic deformation/response, then the response is purely elastic and trivial. If the applied cyclic load is larger than the elastic limit/first yield point and less than a certain elastic shakedown limit, then we get what is known as a plastic shakedown event where plastic deformation ceases after a number of initial cycles and the response goes back to pure elastic with some state of residual stress where P_s is the elastic shakedown limit and P_e is the elastic limit.

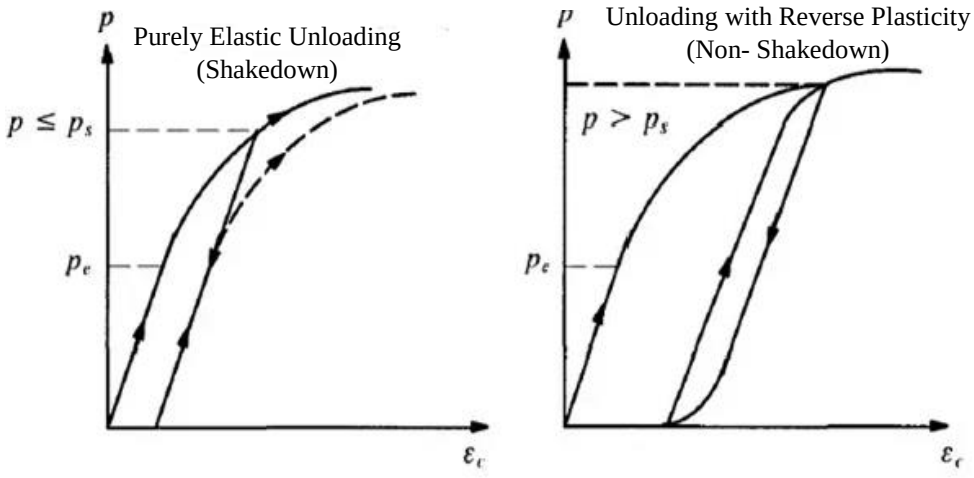

Figure 5.12 Plastic Shakedown behaviour for loading and unloading (Yu 2007)

The longitudinal strain for concrete at peak load and during unloading becomes zero i.e. residual stress at mid span top of the concrete slab is given below.

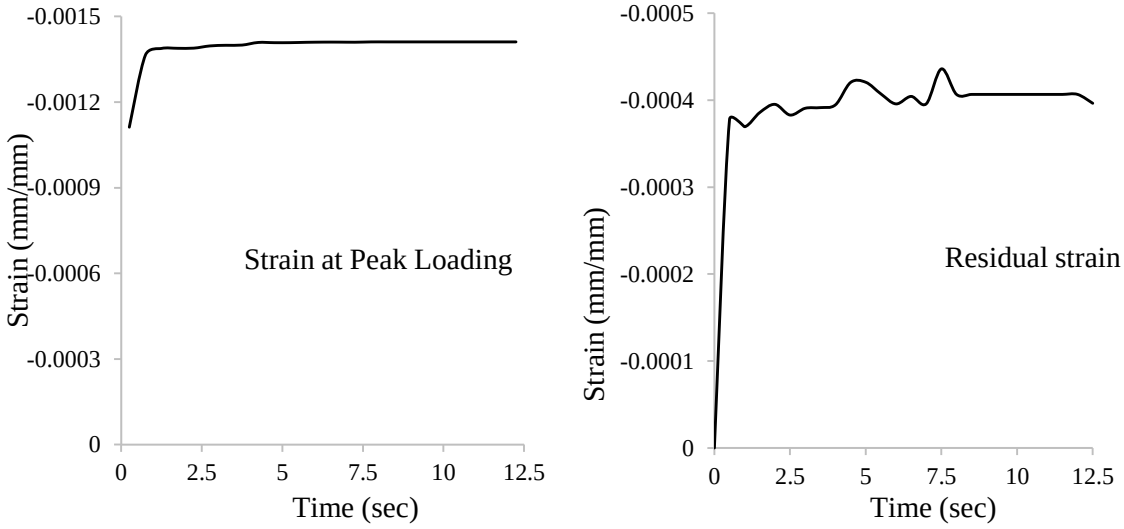

Figure 5.13 Variation of Strain for concrete at peak loading and zero loading for 25 cycles

It is clear from the graph, the longitudinal strain for concrete at peak loading increases with the number of cycles and finally become constant at -0.0014 which is higher than the strain at peak cyclic load found during static analysis i.e. -0.00115 around 21.7 percent higher. This may be due to increase in residual strain which increases with number of cycles and finally become constant.

The stress vs. strain graph of concrete at mid-span top of the concrete slab for 25 numbers of cycle is given below.

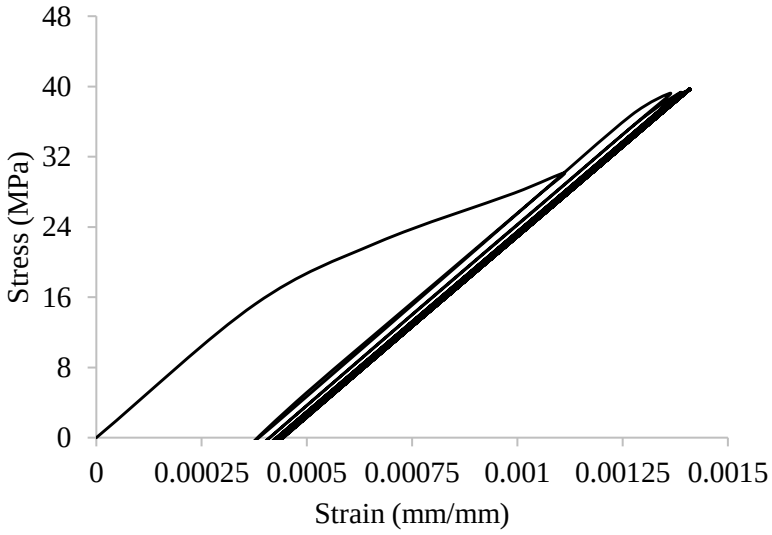

Figure 5.14 Stress vs. Strain Graph of concrete for 25 cycles

5.3 Numerical analysis for 100 numbers of cycles

In the numerical analysis of composite girder under cyclic loading, static general analysis is performed for which Peak Load (L_0) is applied as 450 kN for 100 number of cycles. The time period of each cycle is 0.5 sec thus total time period for 100 cycles will be 50sec. The various parameters such as mid-span deflection of composite girder during peak loading and unloading, residual strain during unloading at bottom of the steel section and at the top of the concrete slab, peak longitudinal stress and strain at the bottom of the steel and at the top of the concrete, reaction at the supports and stress-strain graph for 100 cycles are plotted and compared.

The mid-span deflection of the composite girder at peak loading for 100 number of cycles is given below.

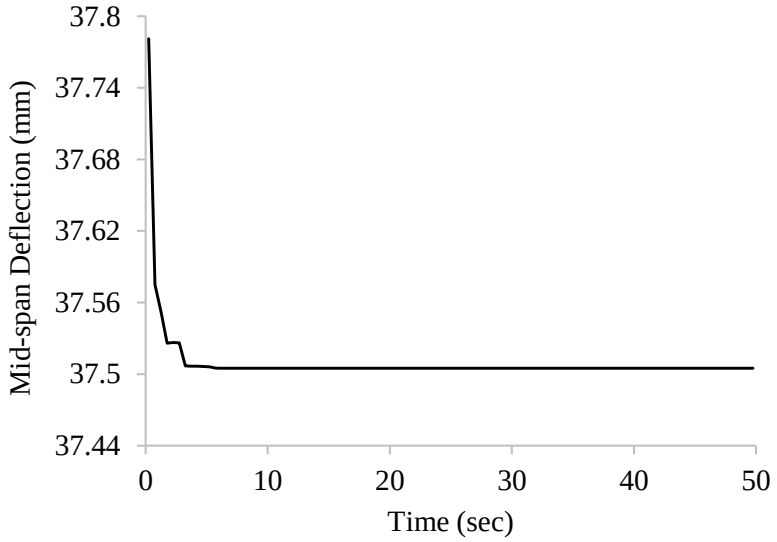

Figure 5.15 Variation of mid-span deflection of composite girder at peak loading for 100 cycles

From graph, it can be shown that initially mid-span deflection of the composite girder is more but as the cycles increases mid-span deflection decreases and finally become constant at 37.50 mm which is lower than the mid-span deflection at peak cyclic load i.e. 39.5 mm found during static analysis. This behaviour may be due to increase in residual deflection of the composite girder during unloading under cyclic loading.

The mid-span deflection of the simply supported composite girder during unloading for 100 number of cycles i.e. residual deflection is given below.

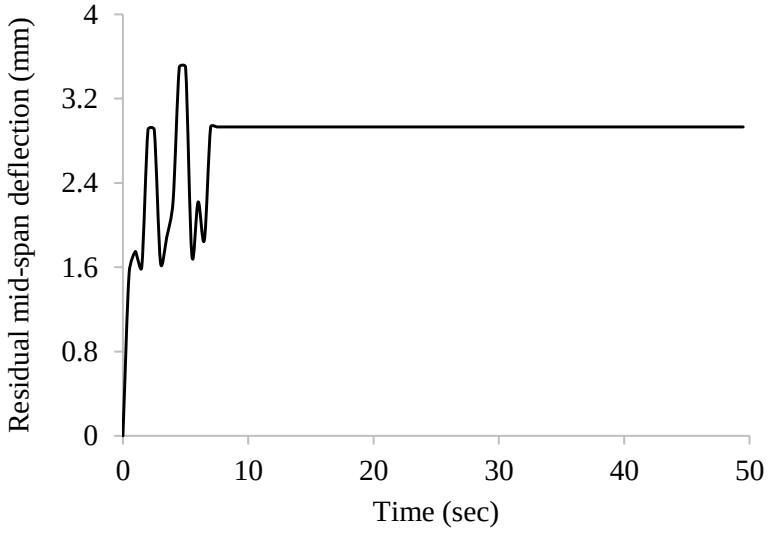

Figure 5.16 Variation of residual mid-span deflection of composite girder for 100 cycles

From the graph, it is clearly shown that residual deflection increases as the number of cycles increases and it became finally constant at 2.93mm which is higher than residual deflection for 25 number of cycles by 2.17 mm i.e. 35 percent more.

The longitudinal stresses at the mid-span bottom of the steel flanges for 100 number of cycles is given below and it can be shown that that it is cyclic in nature.

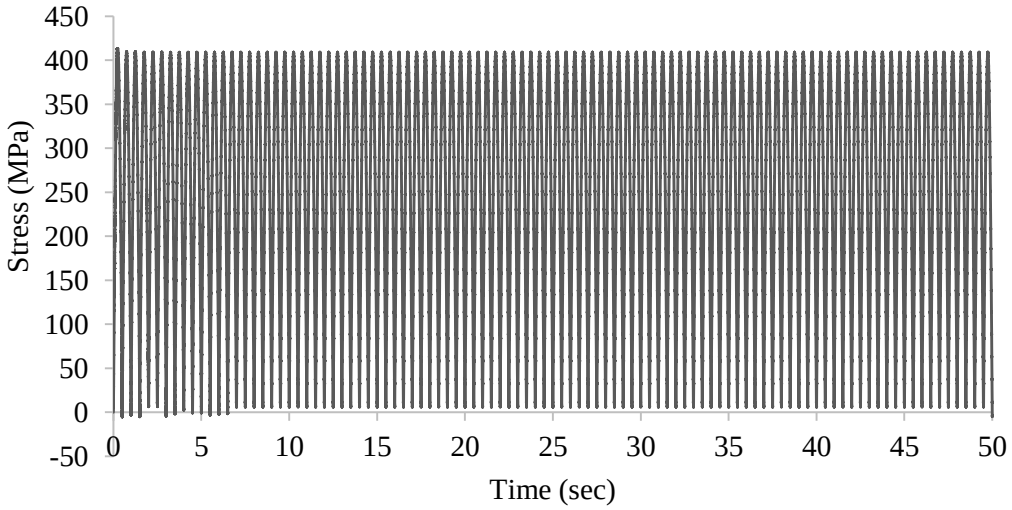

Figure 5.17 Stress vs. Time at mid-span bottom of steel flange for 100 cycle

The longitudinal stresses at the mid-span bottom of the steel flanges and at the mid-span top of the concrete slab during peak loading is shown below.

From the graph, it is clearly shown that longitudinal stresses for steel decrease as the number of cycle increases and finally become constant at 409 MPa which is lower than the longitudinal stress at peak cyclic load i.e. 413.74 MPa found during static analysis whereas for concrete it increases and finally becomes constant at 40 MPa which is lower than at peak cyclic load found during static analysis i.e. 31.17 MPa.

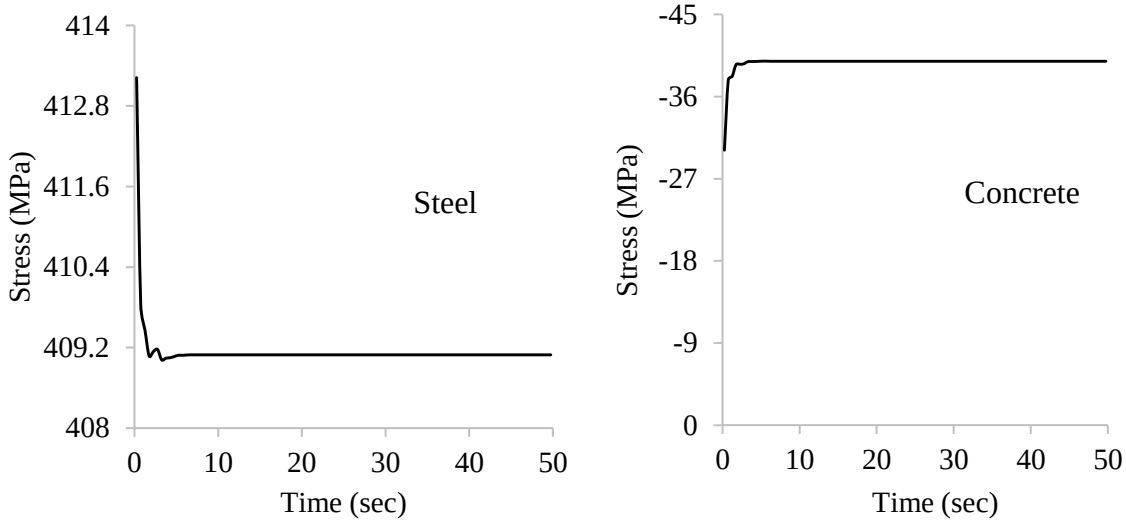

Figure 5.18 Variation of stress for steel and concrete at peak loading for 100 cycles

The longitudinal stresses at mid-span bottom of the steel flanges and at top of the concrete slab are shown below at zero loading l for 100 number of cycles i.e. residual stresses are given below.

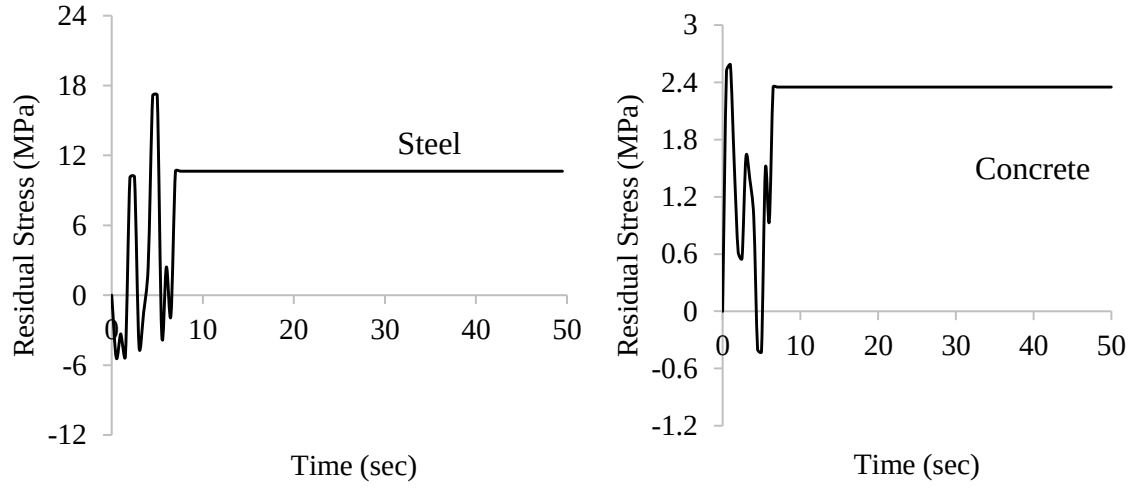

Figure 5.19 Variation of residual stress for steel and concrete for 100 cycles

From the graph, it is shown that residual stress for steel increases as the number of cycles increases and finally becomes constant at 10.65 MPa which is higher than the residual stress for 25 number of cycles i.e. 1.35 MPa by 7.9 times. For concrete residual stress are tensile in nature, increases as the number of cycle increases and finally become constant at 2.35 MPa which is higher than for 25 number of cycles i.e. 1.49 MPa by 1.6 times.

The longitudinal strain at peak loading and the longitudinal strain during unloading for 100 number of cycles i.e. residual strain at mid-span bottom of the steel flange graphs are shown below

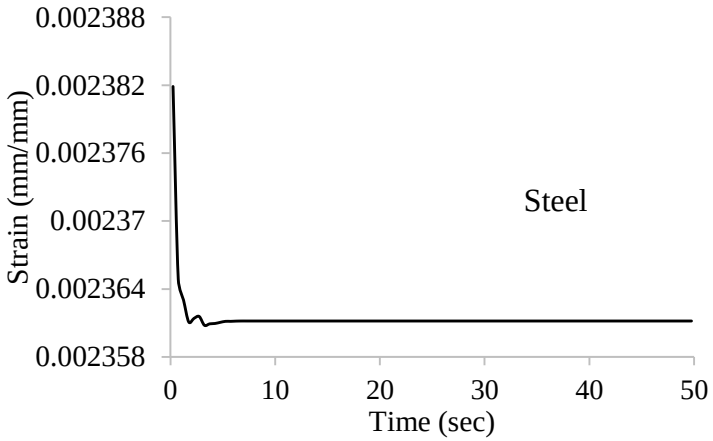

Figure 5.20 Variation of strain for steel at peak loading for 100 cycles

From the graph, it is clearly shown that peak longitudinal strain decreases as the number of cycle increases and finally become constant at 0.002361 which is lower than the longitudinal strain at peak cyclic load i.e. 0.00256 found during static analysis whereas residual strain increases then finally become constant at 0.00037 which is higher than the residual strain for 25 numbers of cycles i.e. 0.00033 by 12.12 percent.

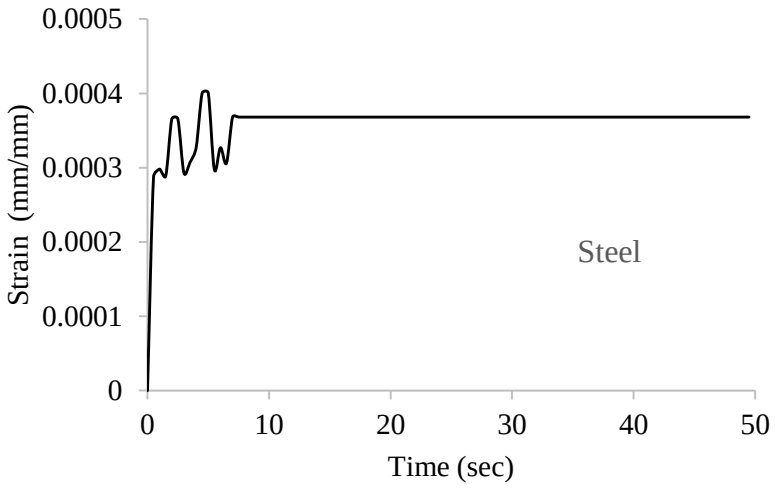

Figure 5.21 Variation of residual strain for steel for 100 cycles

The longitudinal strain for concrete at peak load and during unloading becomes zero i.e. residual stress at mid span top of the concrete slab is given below.

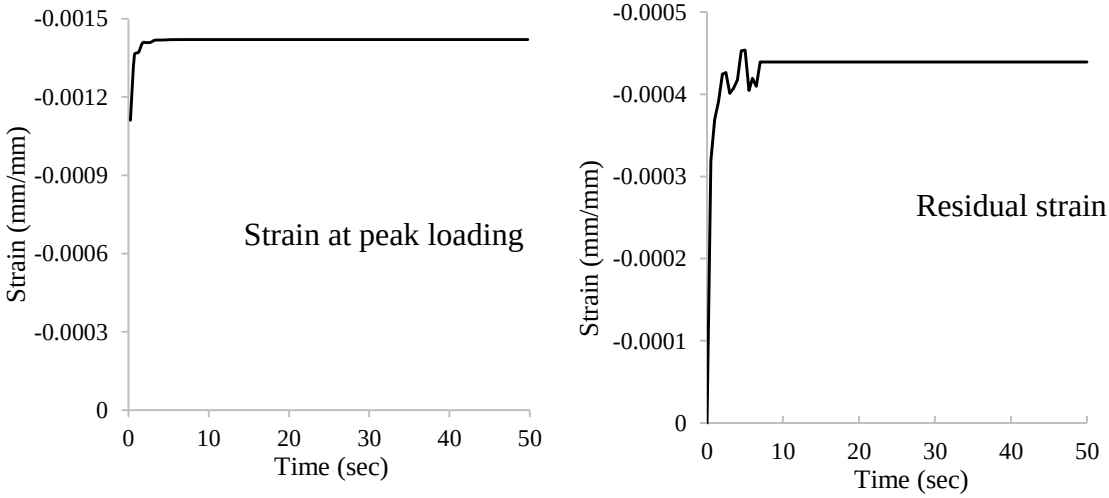

Figure 5.22 Variation of strain for concrete at peak loading and zero loading for 100 cycles

It is clear from the graph, the longitudinal strain for concrete at peak loading increases with the number of cycles and finally become constant whereas residual strain increases with number of cycles and finally becomes constant at -0.00044 which is higher than the residual strain for 25 cycles i.e.-0.0004 by 10 percent more.

The stress vs. strain graph at mid-span top of concrete slab for 100 numbers of cycles is shown below.

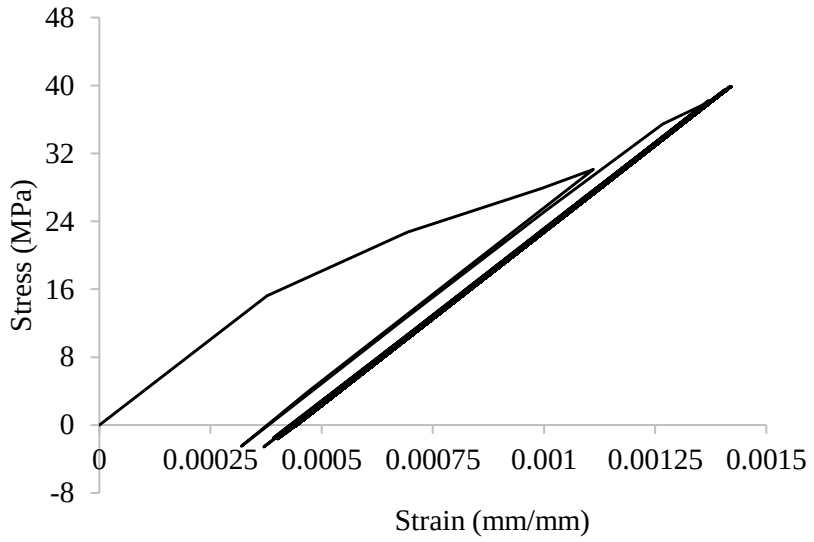

Figure 5.23 Stress vs. Strain Graph for Concrete 100 Cycles

The stress vs. strain graph for concrete under cyclic loading shows the increase in ultimate strain with the increase in the accumulated residual strain. The unloading and reloading curves do not coincide and are not parallel to the initial loading curve. Continuous degradation of the concrete is reflected in the decrease of the slopes of the reloading curves i.e. represents degradation in the modulus of Elasticity. The similar characteristics of stress-strain behaviour of concrete subjected to cyclic loading were obtained in the experimental test performed on concrete by Bahn and Hsu (1998).

The stress vs. strain graph at the mid-span bottom of the steel flange for 100 numbers of cycle is given below.

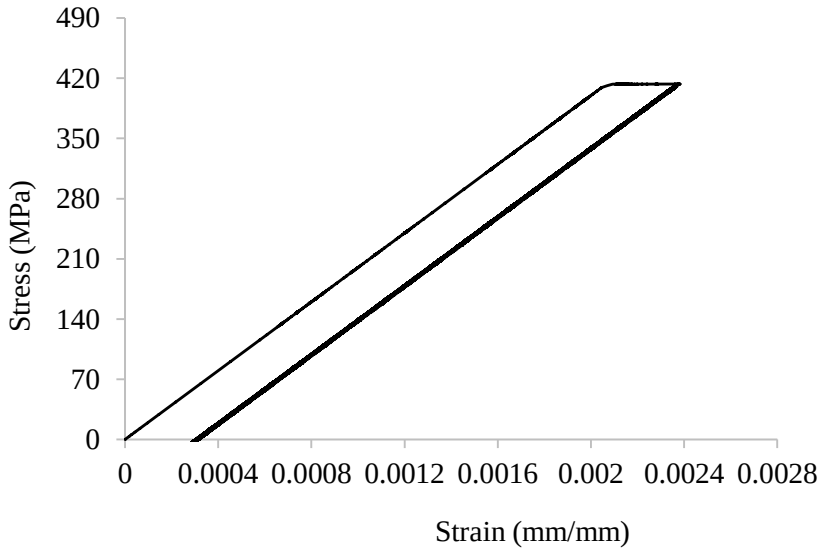

Figure 5.24 Stress vs. Strain graph for steel 100 cycles

The unloading and reloading curves coincide and are parallel to the initial loading curve. This behaviour of stress-strain graph under cyclic loading may be due to plastic shakedown phenomena (Hassan and Kyriakides 1992) explained earlier.

CHAPTER 6

CONCLUSION

6.1 Conclusions

A methodology for finite element modelling of steel-concrete composite girder under cyclic loading has been developed for the numerical analysis of composite girder and its behaviour under cyclic loading as compared to static loading. By computing various parameters above in static loading as well as cyclic loading following conclusions can be drawn

- The actual ultimate load for failure is found to be lowered than the theoretical ultimate load found from the rigid plastic analysis of composite beam in static analysis.
- The stress vs. strain graph for steel under cyclic loading for 25 and 100 number of cycles represents a event where plastic deformation ceases after one cycle and the response goes back to pure elastic with some state of residual stress. The unloading and the reloading curves coincide and parallel to the initial loading curve.
- The stress vs. strain graph for concrete under cyclic loading shows the increase in ultimate strain with the increase in the accumulated residual strain. The unloading and reloading curves do not coincide and are not parallel to the initial loading curve.
- The similar characteristics of stress-strain behaviour of concrete subjected to cyclic loading were obtained in the experimental test performed on concrete in the previo
- The mid-span deflection of the composite beam at peak cyclic load under cyclic loading is found to be less than that under static analysis. This behaviour is due to occurrence of residual mid-span deflection of composite girder.
- Stress and strain produced in steel at peak cyclic load under cyclic loading are less than that of under static loading whereas for concrete both Stress and Strain at peak cyclic load are found to be more that that of under static analysis.
- Residual stress for concrete and steel are tensile in nature, increases as the number of cycles increases and then finally become constant after initial number of cycles. Residual stress and strain after 100 cycles is found to be many times large than that of under 25 cycles.
- The stress and strain for steel along the composite girder at peak loading under cyclic loading decreases as the number of cycles increases and then finally become constant. This may be due to increase in residual stress with the increase in cycles.
- For concrete, the stress and strain at peak cyclic load along the girder under cyclic loading are compressive in nature, increases with the number of cycles and then finally become constant after initial number of cycles.

6.2 Limitations of Study

The present study "Numerical Analysis of Steel-Concrete Composite Girder under Cyclic load" have following limitations

- The number of cycles used for the finite element analysis of composite girder under cyclic loading are well below the cycles used generally in the experimental cyclic tests due to the limitation of computational capacity available for the present study.
- The Steel-concrete composite girder behaviour under cyclic loading with another type of connection such as epoxy-bonded connections or bolted connections are not analysed.
- This study discussed the behaviour of composite girder under cyclic loading with mechanical connection, the same numerical analysis can also be simulated using epoxy bonded connection and its further comparasion can be made with the mechanical connection in the future.

APPENDIX-I: Rigid Plastic Analysis of Composite Girder

Calculations for plastic moment carrying capacity of the steel-concrete composite girder by rigid plastic analysis is shown below.

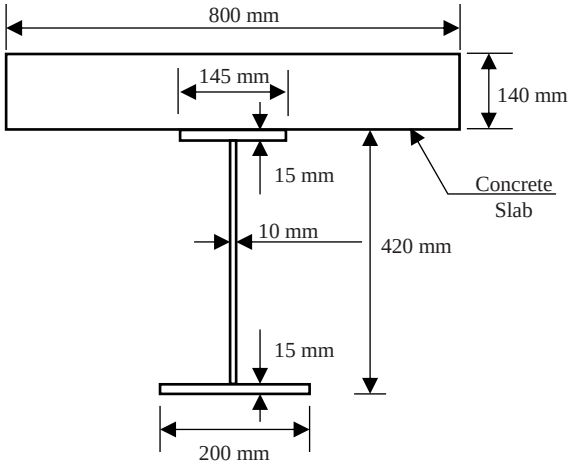

Sectional dimensions of steel-concrete composite girder

Cylindrical compressive strength of concrete (f_c) = 66.7 MPa

Yield strength of steel (f_y) = 413 MPa

Strength of concrete = 0.85*Sectional area of concrete * f_c (7.1)

= 0.85*800 * 140* 66.7

= 6349840 N

= 6349.84 kN

Strength of steel I-section = Sectional area of steel * f_y (7.2)

= (15 * 145 +200*15 + 10*390) * 413

= 3747975 N

= 3747.975 kN

∵ Strength of concrete > Strength of steel

∴ Compressive and tensile forces generated in the plastic state of section will be governed by strength of steel.

Effective depth of concrete in the plastic state = $\frac{\text{Strength of steel}}{\text{width of concrete} * f_c}$ (7.3)

$= \frac{3747975}{800 * 66.7 * 0.85} = 82.63$ mm

Lever for plastic moment = 228.41+140-82.63/2 mm

= 327.095

Plastic moment carrying capacity = Lever arm * Strength of steel (7.4)

= 327.095 * 3747975

= 1.22594 * 10^9 N-mm

= 1225.944 kN-m

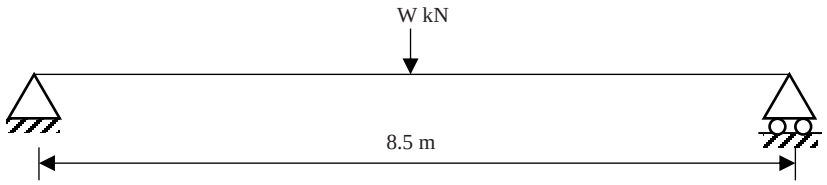

Figure 7.1 Line representation of loads on simply supported composite girder

By equating the maximum bending moment generated in the above beam to the plastic moment carrying capacity of the composite section, collapse load is calculated as

$$\frac{W}{4} * 8.5 = 1225.944 \quad (7.5)$$

From the above equation collapse load W = 576.91 kN

APPENDIX-II: Design of Shear Studs

The design of shear studs in the group is shown below.

Strength of Studs in a group (Oehlers and Johnson 1987) is given by

$$\text{Strength } (D_{max}) = K_{ch} * A_{sh} * f_u * \left(\frac{f_c}{f_u}\right)^{0.35} * \left(\frac{E_c}{E_s}\right)^{0.4} \quad (8.1)$$

Where,

$$K_{ch} = 4.7 - \frac{1.2}{\sqrt{N_{gr}}} \quad (8.2)$$

$$\text{Ngr (number of shear studs in a shear span)} = \frac{\text{Strength of steel}}{D_{max}} \quad (8.3)$$

Ash is the area of the shank of the shear stud.

f_u is the ultimate strength of stud.

f_c is the cylindrical compressive strength of concrete

E_c is modulus of elasticity of concrete

E_s is the modulus of elasticity of stud.

Available data,

$A_{sh} = \frac{\pi}{4} * 19^2 = 283.527$ mm^2

$f_u = 492.05$ MPa

$f_c = 66.7$ MPa

$E_c = 36.6$ GPa

$E_s = 166.488$ GPa

Trial 1,

For first trial assuming N_{gr} as infinity, $K_{ch} = 4.7$

$D_{max} = 177720.317$ N

$N_{gr} = 21.09 \approx 22$

Trial 2,

$K_{ch} = 4.7 - \frac{1.2}{\sqrt{22}} = 4.44$

$D_{max} = 167888.98$ N

$N_{gr} = 22.32 \approx 23$

Trial 3,

$K_{ch} = 4.7 - \frac{1.2}{\sqrt{23}} = 4.449$

$D_{max} = 168258.474$ N

$N_{gr} = 22.27 \approx 23 = N_{gr}$ obtained in previous trial

$\therefore N_{gr} = 23$

Using two parallel rows of shear studs @ 366.591 mm c-c 24 in each row, total no of studs = 24 = 48

Check for spacings

Adopted spacing between rows = 76 mm $\geq 4 * d_{sh}$ (safe)

Adopted edge distance of studs = 25 mm $\geq 1.3 * d_{sh}$ (safe)

Adopted longitudinal spacing between studs = 366.591 mm $\geq 5 * d_{sh}$ (safe)

$\leq 6 *$ depth of concrete (safe)

References

Ameeruthen, M., and Aravindan, S. (2014). "Study Of Stresses On Composite Girder Bridge Over Square and Skew Span." *International Journal of Civil Engineering and Technology*.

Bahn, B. Y., and Hsu, C.-T. T. (1998). "Stress-strain behavior of concrete under cyclic loading." *ACI Materials Journal*, 95, 178-193.

BCSA (2001). "Composite construction." <http://www.steelconstruction.info/Composite_construction>.

Boyer, H. E. (1987). "Atlas of Stress--strain Curves." *ASM International, Metals Park, Ohio 44073, USA, 1987. 630*.

Carreira, D. J., and Chu, K.-H. (1985). "Stress-strain relationship for plain concrete in compression." *ACI Journal*, 82(6), 797-804.

Carreira, D. J., and Chu, K.-H. (1986). "Stress-strain relationship for reinforced concrete in tension." *ACI Journal*, 83(1), 21-28.

Chen, W. F. (1988). "Da Jian Han. Plasticity for Structural Engineers." New York: Springer· Verlag.

Committee, A., Institute, A. C., and Standardization, I. O. f. "Building code requirements for structural concrete (ACI 318-08) and commentary." American Concrete Institute.

Gattesco, N., and Giuriani, E. (1996). "Experimental study on stud shear connectors subjected to cyclic loading." *Journal of Constructional Steel Research*, 38(1), 1-21.

Hassan, T., and Kyriakides, S. (1992). "Ratcheting in cyclic plasticity, part I: uniaxial behavior." *International journal of plasticity*, 8(1), 91-116.

Hibbitt, Karlsson, and Sorensen (2013). *Abaqus 6.13 Online Documentation*, Dassault Systèmes.

Hoeppner, D. W. (2013). "Cyclic Loading and Cyclic Stress." *Encyclopedia of Tribology*, Springer, 691-698.

Kmiecik, P., and Kamiński, M. (2011). "Modelling of reinforced concrete structures and composite structures with concrete strength degradation taken into consideration." *Archives of civil and mechanical engineering*, 11(3), 623-636.

Kumar, P., Chaudhary, S., and Gupta, R. (2017). "Behaviour of Adhesive Bonded and Mechanically Connected Steel-concrete Composite under Impact Loading." *Procedia Engineering*, 173, 447-454.

Kumar, P. T., Reddy, L. S., Kumar, P. T., and Reddy, L. S. (2016). "Experimental Studies on Steel-Concrete Composite Beams in Bending." *International Journal*, 2, 28-35.

Kupfer, H. B., and Gerstle, K. H. (1973). "Behavior of concrete under biaxial stresses." *Journal of the Engineering Mechanics Division*, 99(4), 853-866.

Lebet, J.-P., and Papastergiou, D. (2016). "Steel-Concrete Connections by Adhesion, Interlocking, and Friction for Composite Bridges under Cyclic Loading." *Composite Construction in Steel and Concrete VII*, 632-647.

Liang, Q. Q., Uy, B., Bradford, M. A., and Ronagh, H. R. (2005). "Strength analysis of steel–concrete composite beams in combined bending and shear." *Journal of Structural Engineering*, 131(10), 1593-1600.

Mahmoud, A. M. (2016). "Finite element modeling of steel concrete beam considering double composite action." *Ain Shams Engineering Journal*, 7(1), 73-88.

Mans, P., Yakel, A. J., and Azizinamini, A. (2001). "Full-scale testing of composite plate girders constructed using 485-MPa high-performance steel." *Journal of Bridge Engineering*, 6(6), 598-604.

Mishra, G. (2009). "Steel concrete composite beams." <https://theconstructor.org/structural-engg/steel-concrete-composite-beams/6912/>. (31 March, 2017).

Oehlers, D., and Johnson, R. (1987). "The strength of stud shear connections in composite beams." *The Structural Engineer*, 65(2), 44-48.

Services, C. (2007). "Benefits of Using Reinforced Concrete in Construction | Ocmulgee Concrete Services." <http://ocmulgeeconcreteservices.com/raleigh-services/benefits-of-using-reinforced-concrete-in-construction/>. (6 April 2017).

Wahalathantri, B. L., Thambiratnam, D., Chan, T., and Fawzia, S. "A material model for flexural crack simulation in reinforced concrete elements using ABAQUS." *Proc., Proceedings of the First International Conference on Engineering, Designing and Developing the Built Environment for Sustainable Wellbeing*, Queensland University of Technology, 260-264.

Yu, H.-S. (2007). *Plasticity and geotechnics*, Springer Science & Business Media.

Zhao, G., and Li, A. (2008). "Numerical study of a bonded steel and concrete composite beam." *Computers & Structures*, 86(19), 1830-1838.

Zheng, Y., Robinson, D., Taylor, S., and Cleland, D. (2009). "Finite element investigation of the structural behaviour of deck slabs in composite bridges." *Engineering Structures*, 31(8), 1762-1776.

Numerical Analysis of Steel-Concrete composite girder under cyclic loading

ORIGINALITY REPORT

%20	%12	%14	%5
SIMILARITY INDEX	INTERNET SOURCES	PUBLICATIONS	STUDENT PAPERS

PRIMARY SOURCES

1	"Steel-Concrete Connections by Adhesion, Interlocking, and Friction for Composite Bridges under Cyclic Loading", Composite Construction in Steel and Concrete VII, 2016. Publication	%2
2	Submitted to University of Bradford Student Paper	%1
3	Gattesco, N.. "Experimental study on stud shear connectors subjected to cyclic loading", Journal of Constructional Steel Research, 199605 Publication	%1
4	www.quora.com Internet Source	%1
5	abaqus.ethz.ch:2080 Internet Source	%1
6	etd.lsu.edu Internet Source	%1